

International Journal of Modern Physics A  
 c World Scientific Publishing Company

## BLACK HOLE AND BRANE PRODUCTION IN TEV GRAVITY : A REVIEW

MARCO CAVAGLIA

Center for Theoretical Physics, Massachusetts Institute of Technology  
 77 Massachusetts Avenue, Cambridge MA 02139-4307, USA

and

Institute of Cosmology and Gravitation, University of Portsmouth  
 Portsmouth PO1 2EG, U.K.<sup>†</sup>

In models with large extra dimensions particle collisions with center-of-mass energy larger than the fundamental gravitational scale can generate non-perturbative gravitational objects such as black holes and branes. The formation and the subsequent decay of these super-Planckian objects would be detectable in particle colliders and high energy cosmic ray detectors, and have interesting implications in cosmology and astrophysics. In this paper we present a review of black hole and brane production in TeV-scale gravity.

Keywords: Large extra dimensions; black holes; branes.

### 1. Introduction

In the spring of 1998 Arkani-Hamed, Dimopoulos and Dvali (ADD)<sup>1,2</sup>, later joined by Antoniadis<sup>3</sup>, proposed a possible solution to the hierarchy problem of high-energy physics. In the ADD scenario the electroweak scale ( $E_{EW} \sim 1$  TeV) is identified with the ultraviolet cutoff of the theory. Unification of electroweak and Planck scales takes place at  $\sim 1$  TeV. Gravity becomes strong at the electroweak scale and neither supersymmetry nor technicolor are required to achieve radiative stability. The idea that the gravitational scale can be lowered by some unknown physics dates back to the early 90's when Antoniadis<sup>4</sup> first proposed that perturbative string theories generally predict the existence of extra dimensions at energies of order of the TeV scale. In presence of Large Extra Dimensions<sup>a</sup> (LEDs) the observed weakness of gravity is a consequence of the "leakage" of gravity in the extra dimensions. The Standard Model (SM) fields are constrained in a four-dimensional submanifold of the higher-dimensional spacetime. The success of the SM up to energies of a few hundreds of GeV indeed requires SM fields to be localized on a three-brane embedded in the extra dimensions<sup>5</sup>. On the contrary, gravity and other non-SM fields are allowed to freely propagate outside the three-brane.

<sup>†</sup>Email: marco.cavaglia@port.ac.uk

<sup>†</sup>Present address.

<sup>a</sup>Here "large" means larger than the fundamental scale.

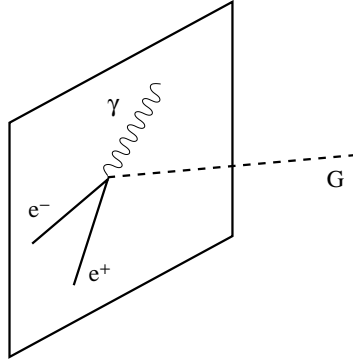


Fig. 1. A schematic illustration of the braneworld model. SM fields are confined to the three-dimensional brane whereas gravitons can propagate in the extra dimensions.

The recognition of the ADD scenario as a *feasible* model of high-energy physics was soon boosted by the possibility of including the ADD model in a consistent theory of Quantum Gravity (QG): String Theory (ST). In the past years ST<sup>6</sup> has emerged as the most successful candidate for a consistent theory of QG. The most recent understanding of ST entails that the five consistent STs and 11-dimensional supergravity (SUGRA) are connected by a web of duality transformations. Type I, II and heterotic STs, and 11-dimensional SUGRA constitute special points of a large, multi-dimensional moduli space of a more fundamental nonperturbative theory, called M-theory. In addition to strings, the nonperturbative formulation of ST predicts the existence of higher-dimensional, nonperturbative extended objects (D-branes)<sup>6</sup>. The presence of branes in the theory leads naturally to the localization of the SM fields and to the hierarchy in the size of the extra dimensions which are postulated in the ADD scenario<sup>b</sup>. Therefore, TeV-scale gravity can be successfully realized in ST<sup>9;10;11</sup>.

The attractiveness of the ADD proposal promptly opened up a whole new field of investigation which is evident in the explosion of papers appeared in the literature. Within months Dienes, Dudas and Gerghetta<sup>12</sup> investigated the effects of extra dimensions on the GUT scale. Giudice, Rattazzi and Wells<sup>13</sup>, and Mirabelli, Perelstein and Peskin<sup>14</sup> studied the consequences of LEDs for high-energy collider experiments. Han, Lykken and Zhang<sup>15</sup>, and Hewett<sup>16</sup>, studied low-energy phenomenology of TeV-scale Kaluza-Klein (KK) modes. Argyres, Dimopoulos and March-Russell<sup>17</sup>, and Kaloper and Linde<sup>18</sup>, investigated the properties of Black Holes (BHs) and inflation in the LED scenario, respectively. Randall and Sundrum proposed an alternative solution to the hierarchy problem based on the existence

<sup>b</sup> In the Horava-Witten model<sup>7;8</sup>, for example, the hierarchy of the extra dimensions and the confinement of the SM fields on a three-brane follow from a double compactification of 11-dimensional SUGRA on a one-dimensional orbifold and on a Calabi-Yau six-fold.

of warped extra dimensions<sup>19;20</sup>. Afterward, the number of papers on the subject has increased dramatically.

The presence of LEDs affects both sub- and super-Planckian physics. Sub-Planckian physics is essentially affected by the presence of KK modes<sup>15;16</sup>. The coupling of KK states to SM particles leads to deviations from SM predictions in perturbative processes such as quarkonium radiative decays, two- and four-fermion interactions and production of gauge bosons. In the LED scenario effective interactions resulting from massive KK modes are suppressed by powers of the fundamental Planck mass  $M_{\text{pl}} \sim O(\text{TeV})$ . This leads to significant experimental signatures. Super-Planckian physics<sup>c</sup> involves non-perturbative effects. The most striking super-Planckian phenomenon is the formation of Non-Perturbative Gravitational Objects (NPGOs) from hard-scattering processes. Creation of BHs from super-Planckian scattering was advocated by Banks and Fischler<sup>25</sup> soon after the appearance of the papers on non-perturbative sub-Planckian effects. Particle collisions with Center-of-Mass (CM) energy larger than the fundamental Planck mass, and impact parameter smaller than the Schwarzschild radius associated with the CM energy, are expected to generate BHs. A completely inelastic process creates a single BH which subsequently decays via Hawking radiation<sup>26</sup> and can be regarded as an intermediate metastable state in the super-Planckian scattering. BH formation is expected to dominate hard-scattering processes because the number of non-perturbative states grows faster than the number of perturbative string states. Moreover, the cross-section for BH formation grows with energy faster than cross-sections of non-perturbative sub-Planckian processes. Formation and evaporation of super-Planckian BHs would be detectable in future hadron colliders<sup>27;28;29;30;31;32</sup> such the Large Hadron Collider (LHC)<sup>33</sup> or the Very Large Hadron Collider (VHLC)<sup>34</sup>. Ultra High-Energy Cosmic Rays (UHECRs) impacting Earth's atmosphere with CM energy of a few hundreds of TeV<sup>35</sup> could also produce transient BHs<sup>36</sup> that would account for features in the spectrum of UHECR<sup>37;38</sup> and be observed in neutrino telescopes<sup>39;40;41</sup>, ground array and air fluorescence detectors<sup>42;43;44</sup>.<sup>d</sup>

If super-Planckian collisions create NPGOs, production of spherically symmetric BHs is just the simplest of a plethora of possible super-Planckian physical processes. At Planckian or super-Planckian energies, we also expect creation of other NPGOs which are predicted by QG theories.

p-branes are p-dimensional spatially extended solutions of gravitational theories in higher dimensions, such as higher-dimensional Einstein-Maxwell theory<sup>47;48</sup> or low-energy effective STs<sup>49;50;51</sup>. They are translationally invariant in p-dimensions and isotropic in the  $D - p - 1$  spatial directions transverse to the translationally-symmetric ones, i.e., p-branes preserve the  $(\text{Poincare})_{p+1} \times \text{SO}(D - p - 1)$  symme-

<sup>c</sup>The physics of super-Planckian collisions has a long history dating back to the late 80's | early 90's. See Refs.<sup>21;22;23;24</sup>.

<sup>d</sup>See Refs.<sup>45;46</sup> for recent and comprehensive reviews.

try. Therefore, they can be viewed as Poincaré-invariant hyperplanes propagating in spacetime. p-branes are characterized by the tension  $T$ , the mass  $M_p$  and a set of conserved charges. They possess naked singularities and/or horizons. In the former case p-brane solutions are interpreted as the exterior metric of higher-dimensional extended objects such as (cosmic) strings<sup>47</sup>. In the latter, they are usually called "black" branes because their geometry is that of a  $(N-p)$ -dimensional hole p-dimensional hyperplane. A 0-brane is a spherically symmetric BH. Branes are a generic phenomenon of any gravitational theory. The presence of extra dimensions is indeed sufficient to permit the existence of these extended objects, though their physical properties depend on the theory. Therefore, if the fundamental Planck scale is of order of TeV, it is reasonable to expect creation of branes at energies above the TeV scale<sup>52;53</sup>. Super-Planckian physics is affected by the production of BHs and p-branes alike. TeV-branes can produce experimental signatures in particle colliders<sup>52;53;54</sup> and in UHECR physics<sup>52;53;55;56;45</sup>. In cosmology, primordial creation of stable branes may have played an important role in the dynamics of the very early universe when the temperature was above the TeV scale; brane relics could be the observed dark matter<sup>53</sup>.

The purpose of this article is to review the theory and the phenomenology of BH and brane production in LED gravity and present an up-to-date bibliography on the subject. In the next section we will review the basic features of TeV-scale gravity and LED models. The physics of brane formation in TeV-scale gravity follows closely that of BHs. Therefore, we first discuss BH creation in LED models in Sect. 3. Sections 4-7 deal with TeV-branes. In Sect. 4 we review brane solutions in Einstein-Maxwell and low-energy STs and discuss their formation and basic properties. Sections 5-7 deal with experimental signatures in particle colliders, UHECRs and cosmology, respectively. Conclusion and outlook complete the review.

## 2. Hierarchy Problem and TeV Gravity

Two different fundamental energy scales are observed in nature: The electroweak scale  $E_{EW} \sim 1$  TeV and the gravitational scale  $E_G \sim 10^{16}$  TeV. The SM of particles successfully explains particle physics up to the  $E_{EW}$  energy. However, little is known about quantum physics above the electroweak scale. One of the most challenging issues is to explain the hierarchy problem, i.e. the largeness and radiative stability of the ratio  $E_G/E_{EW}$ .

### 2.1. Gravity and Extra Dimensions

Classical gravity is described by the Einstein-Hilbert action

$$S_{EH} = \frac{1}{16 G_4 M^2} \int d^4x \sqrt{-g} R(g); \quad (1)$$

where  $M$  is a four-dimensional hyperbolic manifold with metric  $g$ ,  $g$  is the determinant of the metric,  $R(g)$  is the Ricci scalar, and  $G_4 = 6.673(10) \cdot 10^{-11} \text{ m}^3 \text{ kg}^{-1} \text{ s}^{-2}$

$= 6.707(10) \cdot 10^{39} \text{ hc } (G \text{ eV} = c^2)^{-2}$  is the gravitational constant (Newton's constant). In natural units  $G_4$  has dimensions of inverse mass squared. The Planck mass

$$M_{\text{Pl}} = G_4^{-1/2} = 1.22 \cdot 10^{\frac{D-2}{2}} \text{ TeV} \quad (2)$$

determines the gravitational scale at which quantum gravitational phenomena become strong. At low energy, gravity manifests itself as a long-range attractive force with coupling constant  $G_4$ . The gravitational potential of a massive object with mass  $M$  at a distance  $r$  is

$$V(r) = -G_4 \frac{M}{r} \quad (3)$$

Experiments with a torsion pendulum /rotating attractor instrument<sup>57;58</sup> have recently tested the gravitational force at length scales below 1 mm without evidence for violations of Eq. (3).

Any consistent theory of QG must reduce to the Einstein-Hilbert theory in the low-energy limit. ST requires that we live in a higher-dimensional spacetime. In the Einstein frame, the generic bosonic sector of low-energy effective STs is described by the action

$$S = \frac{1}{16 G_D} \int D^D x^P \sqrt{-g} R(g) - a(x)^2 \frac{1}{2n!} e^b F_{[n]}^2 + \text{CS terms} \quad (4)$$

where  $\phi$  is a scalar field (dilaton),  $F_{[n]}$  is the field strength of the  $(n-1)$ -form gauge potential  $A_{[n-1]}$  and  $D = 10$  or  $11$ . The parameters  $a$ ,  $b$  and  $n$ , and the Chern-Simons (CS) terms, depend on the model. For instance, 11-dimensional SUGRA has  $a = b = 0$ ,  $n = 4$  and CS terms equal to  $\frac{1}{6} F_{[4]} \wedge F_{[4]} \wedge A_{[3]}$ . If ST is the ultimate theory of QG, six or seven dimensions must be compactified to yield a four-dimensional effective action. This is generally accomplished by assuming that the higher-dimensional spacetime is a (warped) product of four-dimensional Minkowski spacetime and a compact  $(D-4)$ -dimensional Riemannian manifold. The spacetime metric is

$$ds^2 = g_{ab}(x) dx^a dx^b = e^{2A(y)} dx^\mu dx^\nu + h_{ij}(y) dy^i dy^j \quad (5)$$

where the Greek indices run from 0 to 3 and the coordinates  $y$  ( $i, j = 4 :: D-1$ ) parametrize the compactified dimensions. In such a scenario, the observed Planck scale  $M_{\text{Pl}}$  is a quantity derived from the  $D$ -dimensional fundamental Planck scale<sup>e</sup>

$$M_{\text{Pl}} = G_D^{-1/(D-2)} \quad (6)$$

The four-dimensional Newton's constant is related to the  $D$ -dimensional gravitational constant  $G_D$  by the relation

$$G_4 = \frac{G_D}{V_{D-4}} \quad ; \quad M_{\text{Pl}}^2 = M_{\text{?}}^{\frac{D}{2}} V_{D-4} \quad (7)$$

<sup>e</sup>For notations see Appendix A.

where

$$V_{D-4} = \int d^D y \frac{1}{h} e^{2A(y)} \quad (8)$$

is the volume of the extra-dimensional space modulated by the warp factor  $e^{A(y)}$ . The ratio of the fundamental Planck constant  $M_{\text{Pl}}$  to the observed Planck constant  $M_{\text{Pl}}$  depends on the geometry and on the size of the compactified space. If the volume of the latter is of order of the fundamental Planck scale, then all quantities in Eq. (7) are of order  $10^{16}$  TeV. However, other scenarios are possible: In the Horava-Witten model, for instance,  $M_{\text{Pl}}$  is of order of the GUT scale.

Equation (7) provides a possible solution to the hierarchy problem, which is bypassed by identifying  $M_{\text{Pl}}$  with the electroweak scale. The volume of the extra-dimensional space is large in fundamental Planck units. For instance, assuming for simplicity a symmetric toroidal compactification with radii  $R_i = L/2$  the condition  $M_{\text{Pl}} = M_{\text{EW}}$  gives the relation:

$$L = 10^{30-n} \text{ cm} \frac{\text{TeV}}{M_{\text{EW}}}^{1+2=n}; \quad (9)$$

where  $n = D - 4$  is the number of extra dimensions. An upper limit to the size of the compactified space can be obtained by measuring the gravitational potential at small distances. Indeed, if  $n$  extra dimensions open up at the scale  $L$ , the gravitational potential at scales smaller than  $L$  behaves as

$$V(r) \sim G_{n+4} \frac{M}{r^{n+1}}; \quad (10)$$

Clearly, the non-observation of deviations from the four-dimensional behavior of Eq. (3) at a distance  $L^0$  constrains the size of the extra dimensions and the fundamental Planck scale to be larger than  $L^0$  and  $L^{0-1}$ , respectively. The latest experimental results<sup>58</sup> suggest that the gravitational force follows the inverse square law up to distances of 150  $\mu\text{m}$ . For a two-dimensional symmetric toroidal compactification this implies a fundamental Planck scale  $M_{\text{Pl}} > 1.6$  TeV.

## 2.2. Theoretical Models

A lot of efforts have been devoted to the formulation of LED models in ST and M-theory (see, e.g., Ref.<sup>59</sup> for a short review). Although the LED scenario does not require ST, the two main ingredients of TeV gravity, namely the hierarchy of scales and the confinement of the SM fields on a three-branes, can be easily accommodated in ST.

### 2.2.1. Heterotic String Theory

In weakly coupled heterotic ST, the relation between the four-dimensional Planck scale and the string scale  $M_s$  is

$$M_{\text{Pl}}^2 = \frac{1}{2} M_s^8 V_6 = \frac{1}{g^2} M_s^2; \quad (11)$$

where  $V_6$  is the volume of the compactified space,  $\langle \phi \rangle = e^{h_i} - 1$  is the vacuum expectation value of the dilaton field, and  $g$  is the gauge coupling. Since  $g \approx 1=5$  the heterotic string scale appears to be near the Planck scale. The string is weakly coupled when the compactified volume is of order of the string scale. However, in order to break supersymmetry by compactification at a scale smaller than the heterotic string scale, a large compactification radius is needed. In this case  $\langle \phi \rangle$  becomes large and ST is strongly coupled. Strongly coupled ST can be discussed by means of dualities. For instance, strongly coupled ST with one (two or more) large radii is given by weakly coupled type IIB (IIA or I/I') ST. In the strongly coupled regime Eq. (11) is no more valid. The string tension becomes an arbitrary parameter which can provide a solution to the hierarchy problem.

### 2.2.2. Type I/I' String Theory

A consistent framework for realizing the ADD scenario is type I ST. The strongly coupled regime of SO(32) heterotic ST is given by type I or I' ST. In type I/I' ST closed and open strings describe gravity and gauge fields, respectively. The SM fields are confined on a collection of D p-branes, where the ends of the open strings are constrained to propagate<sup>3;11</sup>. The Planck scale and the gauge coupling are

$$M_{P1}^2 = \frac{1}{2} M_s^8 V_L V_T; \quad g^2 = \frac{1}{s} M_s^{p-3} V_L; \quad (12)$$

where  $V_L$  and  $V_T$  are the volume of the  $(p-3)$ -dimensional longitudinal space and the volume of the  $(9-p)$ -dimensional transverse space to the D p-brane, respectively. Calculability at perturbative level ( $s < 1$ ) requires that the  $p-3$  longitudinal dimensions are compactified on the string scale. For a symmetric transverse compactification with radius  $R_T$ , Eq. (12) gives

$$M_{P1}^2 = \frac{1}{g^4 v_L} M_s^{11} v_R^{9-p}; \quad (13)$$

where  $v_L \approx 1$  is the longitudinal volume in string units. If the  $9-p$  transverse dimensions are compactified on a much larger scale than the string scale  $M_s$ , the string scale can be smaller than the Planck scale. Therefore, gravity becomes strong at a much lower scale ( $M_s$ ) than the Planck scale, though the string is weakly coupled.

### 2.2.3. Type IIA/IIB String Theory

Heterotic ST compactified to six or less dimensions admits a dual description as a type II ST. The gauge coupling is independent from the string coupling  $g_s$ . Let us consider for simplicity a compactification on  $K3 \times T^2$ . For type IIA ST we have

$$M_{P1}^2 = \frac{1}{2} M_s^2 v_K^2 v_{T^2}; \quad g^2 = v_{T^2}; \quad (14)$$

where  $v_{K3}$  and  $v_{T^2}$  are the volume of the Calabi-Yau and of the two-torus in string units, respectively. The second relation implies  $v_{T^2} = 1$ . The Planck scale is

$$M_{Pl}^2 = \frac{1}{g^2} \frac{v_{K3}}{2} M_s^2 : \quad (15)$$

In the previous equation the volume of the Calabi-Yau manifold and the string coupling are free parameters. We can lower the string scale either by choosing a large  $K3$  volume or a small string coupling  $g_s = 10^{14,60,61}$ . In the latter scenario, gravity remains weak up to the Planck scale. Therefore, there are no observable quantum gravitational effects at the TeV scale.

For type IIB ST we have

$$M_{Pl}^2 = \frac{1}{2} M_s^2 v_{K3} v_{T^2} ; \quad g^2 = \frac{R_1}{R_2} ; \quad (16)$$

where  $R_1$  and  $R_2$  denote the radii of the two-dimensional torus. Setting  $R_2 = g^2 R_1$ , the relation between the Planck scale and the string scale is

$$M_{Pl} = \frac{g}{s} v_{K3}^{1/2} R_1 M_s^2 : \quad (17)$$

The largest value for the string scale  $M_s = 10^6$  TeV is obtained by choosing  $R = 1$  TeV and  $v_{K3} = 1$ .

#### 2.2.4. M-theory

Strongly coupled  $E_8 - E_8$  ST compactified on a Calabi-Yau six-fold  $CY_6$  is described by 11-dimensional SUGRA compactified on  $S^1 = Z_2 - CY_6$ . It follows that

$$M_{Pl}^2 = V_{CY} R_{11} M_s^9 ; \quad g^2 = V_{CY} M_s^6 ; \quad (18)$$

where  $V_{CY}$  is the volume of the Calabi-Yau six-fold and  $R_{11}$  is the radius of the orbifold. Setting  $M_s = 1$  TeV we obtain  $R_{11} = 10^{11}$  m, which is excluded experimentally. The lowest value of the M-theory scale which is experimentally admissible is  $M_s = 10^4$  TeV, corresponding to  $R_{11} = 1$  mm.

Table 1. Possible LED scenarios in ST/M-theory. The first two columns give the number of LEDs and Small Extra Dimensions (SEDs)  $M_s^{-1}$ . The third column gives the string/M-theory scale  $M_s$ .

	LED	SED	$M_s$
I/I' ST	n = 2 (fm { mm )	6 = n	TeV
IIA ST	2 = n = 4 (fm { mm )	6 = n	TeV
IIB ST	2 ( fm )	4	$10^6$ TeV
M-theory	1 (< mm)	6	$> 10^4$ TeV

### 2.2.5. String Theory and Warped Metrics

Warped metrics arise naturally in STs thanks to the presence of D-branes. (See, e.g., Refs. <sup>62;63</sup> for recent reviews.) A simple example of D-brane-induced warping has been given by Verlinde <sup>64</sup> who considers a stack of  $N$  D3-branes with geometry  $AdS_5 \times S^5$ , where the  $AdS_5$  submanifold is represented as the warped product of a Poincare-invariant four-dimensional spacetime and a radial direction. The Verlinde model has recently been extended in Ref. <sup>65</sup>.

### 2.3. Phenomenology of Compactification Models

In this section we briefly discuss a few simple examples of compactification. At a phenomenological level, the  $n$ -dimensional internal space is characterized by the existence of one or more compactification scales. The metric of the spacetime is given in Eq. (5). Compactifications are divided in two categories: Factorizable ( $A(y) = 0$ ) and non-factorizable or "warped" ( $A(y) \neq 0$ ).

#### 2.3.1. Toroidal Compactifications

The simplest example of factorizable compactification is the  $n$ -torus ( $h_{ij} = R_i \delta_{ij}$ ,  $y_i \in [0; 2\pi]$ ). If all the radii  $R_i$  have the same size  $R$ , the toroidal compactification is called symmetric. The ratio between the Planck scale and the fundamental scale is:

$$\frac{M_{Pl}^2}{M_*^2} = \frac{L^0}{L_*} \quad l_*^n; \quad (19)$$

where  $L^0 = 2\pi R$  and  $L_* = M_*^{-1}$ . ST seems to favor the existence of more than one compactification scale. In the simplest scenario with  $m < n$  extra dimensions compactified on the  $L$  scale and  $n - m$  dimensions compactified on the  $L^0$  scale we have

$$\frac{M_{Pl}^2}{M_*^2} = l_*^m l_*^{n-m}; \quad (20)$$

If  $L = L_*$ , Eq. (20) reduces to Eq. (19) with  $n - m = n$ . Therefore, experimental constraints for the  $n$ -dimensional symmetric model apply also to the asymmetric model with  $n - m$  large dimensions. A symmetric compactifications in the LED context were first discussed by Lykken and Nandi <sup>66</sup>.

#### 2.3.2. Fat Branes and Universal Extra Dimensions

In the compactification models considered above, the SM particles are constrained to propagate on three-dimensional branes of infinitesimal thickness. However, for asymmetric compactifications with small extra dimensions, we can think of a scenario in which the SM particles propagate in spatial dimensions other than the macroscopic ones.

In the Fat Brane (FB) model the three-brane can be thought as a thick wall, with the SM particles propagating inside the wall. The FB model was first discussed by Arkani-Hamed and Schmaltz (AS) in Ref. <sup>67</sup>. In the AS scenario the wall is thick in one dimension. The Higgs and the SM gauge fields are free to propagate inside the wall whereas the SM fermions are stuck at different depths in the wall. Therefore, fermions and gauge fields "see" three and four spatial dimensions, respectively. If the wall thickness is of order of the TeV<sup>-1</sup> scale, the AS model leads to interesting perturbative effects that would be detectable at future particle colliders.

In the Universal Extra Dimension (UED) scenario <sup>68</sup> all SM particles are allowed to propagate freely in some of the extra dimensions, provided that these dimensions are smaller than a few hundreds of GeV<sup>-1</sup>. A peculiar feature of the UED model is that the KK excitations are produced in groups of two or more. This leads to different signatures in particle collider experiments.

### 2.3.3. Randall-Sundrum Compactification

The simplest example of a warped compactification is the Randall-Sundrum (RS) model <sup>19,20</sup>. The RS spacetime is five-dimensional. The metric is

$$ds^2 = e^{2kr_c y} (dx^2 + r_c^2 dy^2); \quad (21)$$

where  $k$  is a parameter of order of the fundamental Planck scale and  $r_c$  is the radius of the finite-size extra dimension (orbifold)  $y \in [0, y_c]$ . The RS metric (21) is a solution of five-dimensional Einstein gravity coupled to a negative cosmological constant and to two three-branes located at the fixed points of the orbifold:

$$S = \frac{M_5^3}{16} \int dx^4 dy \sqrt{-g} (R - 2\Lambda) + \sum_{i=1,2} \int dx^4 \sqrt{-h^{(i)}} L^{(i)} - V^{(i)}; \quad (22)$$

where  $h^{(i)}$ ,  $L^{(i)}$  and  $V^{(i)}$  are the four-dimensional metric, Lagrangian density, and vacuum energy of the  $i$ -th brane, respectively. The bulk spacetime is a slice of the five-dimensional Anti-de Sitter (AdS) geometry with curvature  $-k^2$ . The bulk cosmological constant and the brane vacuum energy depend on the scale  $k$ :

$$V_1 = -V_2 = \frac{3}{4} M_5^3 k; \quad \Lambda = -12k^2; \quad (23)$$

Thus the branes have opposite tension. The scale  $k$  is smaller than the fundamental scale, i.e., the AdS curvature is small in fundamental units. The radius of the orbifold is small but larger than  $k^{-1}$  so that  $r_c k \gg 1$ . Using Eqs. (7) and (8) we find that the relation between the observed Planck mass and the fundamental Planck mass is

$$M_{Pl}^2 = \frac{M_5^3}{k} \int_0^{y_c} e^{2kr_c y} dy = \frac{M_5^3}{k} \left( \frac{e^{2kr_c y_c} - 1}{2kr_c} \right); \quad (24)$$

The scale of the physical phenomena on the branes is fixed by the value of the warp factor. On the brane located at  $y = y_c$  (visible brane), the conformal factor of the

metric is  $ds^2 = e^{2kr_c} dx^2$  and all physical masses are rescaled by a factor  $e^{-kr_c}$ . If  $kr_c \sim 12$  physical mass scales of order of TeV are generated from a fundamental Planck scale  $10^6$  TeV. Alternatively, the TeV scale can be regarded as the fundamental scale and the Planck mass as the derived scale.

The second RS model<sup>20</sup> is obtained from Eq. (21) by letting  $y_c \rightarrow 1$ . The negative tension brane is located on the AdS horizon and the model formally contains a single brane.

#### 2.4. Experimental Constraints

The size of the extra dimensions and the value of the fundamental Planck scale are constrained by experiments. The constraints for non-warped symmetric toroidal compactifications have been extensively studied in the literature.<sup>f</sup> These constraints can immediately be extended to the asymmetric toroidal compactification with smaller scale of order of the fundamental Planck length.

We have already seen that experiments with a torsion pendulum<sup>57;58</sup> limit the size of  $n = 2$  LEDs to 150  $\mu$ m and the value of  $M_*$  to be larger than 1.6 TeV. A lower bound on the value of the fundamental Planck scale can also be derived from particle collider experiments and astrophysical and cosmological considerations.

##### 2.4.1. Particle Collider Experiments

The particle collider experiments are divided in two categories: non-perturbative and perturbative. The former involves creation of super-Planckian NPGOs such as BHs<sup>25</sup> and branes<sup>52</sup>, and will be discussed in the following sections. The latter consists essentially in missing-energy experiments (due to emission of a real graviton) or search for deviations from SM predictions in fermion-fermion interactions (due to virtual graviton exchange)<sup>13;69;71</sup>. In missing-energy experiments, the idea is to look for processes in which a graviton is scattered off the brane, as in Fig. 1. The deviations from the SM expectations due to the missing momentum carried with the graviton are model-independent<sup>72</sup> and can be measured. The simplest processes of this kind are<sup>69</sup>

$$e^+e^- \rightarrow G; \quad q\bar{q} \rightarrow gG; \quad (25)$$

where  $G$  is a graviton. In the first process, the smoking gun would be the observation of a single photon with missing energy in a  $e^+e^- \rightarrow \gamma + (\text{invisible})$  background<sup>73;71</sup>. The current and future lower bounds on the fundamental Planck scale due to real graviton emission have been given by Cullen et al in Ref.<sup>72</sup> (see Table 2).

The limits on the fundamental Planck scale from virtual graviton effects have been given by L3<sup>74</sup>, ALEPH<sup>75</sup>, DELPHI<sup>76</sup>, OPAL<sup>77</sup>, H1<sup>78</sup> and D0<sup>79</sup> collaborations for various processes. The most stringent bound comes from the D0 experiment and is given in Table 3.

<sup>f</sup>For recent reviews see, e.g., Refs. <sup>69;70;71</sup>.

Table 2. Lower bounds (95% c.l.) on the fundamental Planck scale  $M_{\text{?}}$  (TeV) from missing-energy experiments at present (LEP, Tevatron) and future (LC, LHC) particle colliders for 2-4- and 6-dimensional symmetric toroidal compactifications.

	n=2	n=4	n=6
Lep II	0.90	0.33	0.18
Tevatron	0.86	0.39	0.27
LC	5.8	2.0	1.1
LHC	9.4	3.4	2.1

Table 3. Lower bounds (95% c.l.) on the fundamental Planck scale  $M_{\text{?}}$  (TeV) from virtual graviton exchange processes for n-dimensional symmetric toroidal compactifications (D0 collaboration).

n	2	3	4	5	6	7
$M_{\text{?}}$	0.88	0.77	0.58	0.47	0.39	0.35

#### 2.4.2. Astrophysical and Cosmological Constraints

The astrophysical constraints on  $M_{\text{?}}$  are derived from the study of supernova cooling and neutron star heat excess. In the cooling process of type-II supernovae, the SM predicts that most of the energy is radiated through neutrino emission. In the LED scenario, the KK modes created through gravibremstrahlung processes can also carry energy away. In order to avoid overcooling, the fundamental Planck scale must be not too small. Lower bounds on  $M_{\text{?}}$  have been estimated by Cullen and Perelstein in Ref. <sup>80</sup> (and subsequently refined by several other authors in Refs. <sup>81;82;83</sup>). Using data from the supernova SN 1987A, Cullen and Perelstein give a lower bound of  $M_{\text{?}} > 38, 2.2,$  and  $0.45$  TeV for  $n = 2, 3,$  and  $4$  extra dimensions, respectively. <sup>9</sup> The limits from supernova cooling are much stronger than the limits from collider experiments for  $n = 2;3$  but become unimportant for higher  $n$  <sup>72;69</sup>. However, it should be stressed that the results based on supernova cooling are affected by large uncertainties on the temperature and on the density of the stellar core at collapse. The bounds on  $M_{\text{?}}$  from neutron star heat excess are estimated by constraining the heating process of neutron stars due to the decay and the subsequent absorption of KK gravitons <sup>84</sup>. The lower limit on  $M_{\text{?}}$  is  $\sim 1260$  (33) TeV for  $n = 2$  (3). This result is also affected by large theoretical and experimental uncertainties.

The cosmological constraints on  $M_{\text{?}}$  are derived from the physics of the Cosmic Microwave Background Radiation (CMBR) and of the Cosmic Gamma-Ray Background Radiation (CGRBR). In the former, a lower bound on  $M_{\text{?}}$  is estimated by constraining the cooling rate of the CMBR. The presence of primordial KK gravitons increases the amount of matter in the universe, leading to a more rapid cooling <sup>85</sup>. This sets the lower bounds  $M_{\text{?}} > 65 \{ 750, 4 \{ 32$  and  $0.7 \{ 4$  for  $n = 2,$

<sup>9</sup>Hannestad and Raelt <sup>83</sup> give the more restrictive bounds  $M_{\text{?}} > 63$  (3.9) TeV for  $n = 2$  (3).

3 and 4, respectively. The presence of KK gravitons leads to modifications in the CGRBR. Primordial KK modes can decay in photons and affect the CGRBR. This sets a bound on the primordial nucleosynthesis normalcy temperature which leads to  $M_{\text{pl}} > 83 \{ 263 (2.8 \{ 7.6) \text{ TeV}$  for two (three) LEDs<sup>86</sup>. Constraints derived from overclosure of the universe due to KK modes are generally weaker.

Summarizing, in the toroidal compactification scenario particle collider experiments and astrophysical and cosmological observations can be used to set a lower bound on the fundamental Planck scale. The constraints from astrophysics and cosmology dominate over the constraints derived from particle collider experiments for  $n = 2; 3$  LEDs, though they are affected by larger uncertainties. The estimated bounds on  $M_{\text{pl}}$  seem to rule out a scenario with two (and possibly three) large extra dimensions. Weaker constraints from particle collider experiments dominate for higher-dimensional compactifications.

### 3. Black Holes and TeV Gravity

In the previous section we have discussed the experimental signatures of LEDs in sub-Planckian physics. In this regime gravity is perturbative. Low-scale gravity manifests itself as KK modes which couple to SM fields. When energies reach the fundamental Planck scale, gravity becomes non-perturbative and quantum gravitational effects become strong. ST is believed to describe super-Planckian gravitational processes. Thus it is reasonable to expect that super-Planckian particle collisions produce NPGOs which are predicted by ST, such as BHs, string balls<sup>87</sup>, and branes. In the LED scenario this occurs for processes with energy of order of the TeV scale. At energies well above the Planck scale gravity becomes semiclassical. The entropy of the processes is  $S \gg 1$  and gravitational interactions are described by low-energy effective gravitational theories, such as the Einstein-Hilbert theory (1) or SUGRA theories (4). Therefore, production of NPGOs which are created in hard processes with CM energy  $E_{\text{CM}} \gg M_{\text{pl}}$  can be described by semiclassical gravitational theories, just as gravitational collapse is described by general relativity.<sup>h</sup>

Table 4. Regimes and phenomenology of gravity as a function of the energy. As is explained in the text, at super-Planckian energies we expect formation of NPGOs that are described by semiclassical low-energy gravitational theories.

Energy	Gravity regime	QG effects	Theory	Phenomenology
$E_{\text{CM}} < M_{\text{pl}}$	perturbative	no	SM + KK theory	KK states
$E_{\text{CM}} \sim M_{\text{pl}}$	non-perturbative	yes	Strings/M-theory	String balls/Branes?
$E_{\text{CM}} > M_{\text{pl}}$	non-perturbative	no	Einstein/Sugra	BHs/p-Branes

<sup>h</sup>Formation of NPGOs by inelastic super-Planckian collisions can be thought as asymmetric gravitational collapse.

### 3.1. Super-Planckian BHs

BH formation is a generic non-perturbative process of any gravitational theory. A BH smaller than the size of all LEDs sees a  $D$ -dimensional isotropic spacetime, thus is spherically symmetric. A non-rotating spherically symmetric BH is described by the  $(n+4)$ -dimensional Schwarzschild solution:

$$ds^2 = -R(r)dt^2 + R(r)^{-1}dr^2 + r^2 d_{n+2}^2; \quad (26)$$

where

$$R(r) = 1 - \frac{r_s^{n+1}}{r^{n+1}}; \quad (27)$$

The Schwarzschild radius  $r_s$  is related to the mass  $M_{BH}$  by the relation

$$r_s = \frac{1}{\sqrt{2}} \frac{M_{BH}^{\frac{1}{n+1}}}{M_{\text{pl}}^{\frac{1}{n+1}}}; \quad (28)$$

where

$$n = \frac{8}{2} \frac{\frac{n+3}{2}}{(2+n)}; \quad (29)$$

BHs with mass  $M_{BH} \ll M_{\text{pl}}$  have Schwarzschild radius  $r_s \ll M_{\text{pl}}^{-1}$ . In symmetric compactification models the size of extra dimensions is much larger than  $M_{\text{pl}}^{-1}$ . Therefore, the spherical approximation is justified. The latter breaks down for asymmetric compactifications with some of the extra dimensions of order of the fundamental Planck scale. In this case the geometry of non-perturbative objects is that of black strings and branes. A BH with angular momentum  $J$  is described by the Kerr solution. Equation (28) is substituted by

$$r_s = \frac{1}{\sqrt{2}} \frac{M_{BH}^{\frac{1}{n+1}}}{M_{\text{pl}}^{\frac{1}{n+1}}} \left[ 1 + \frac{(n+2)^2 J^2}{4 r_s^2 M_{BH}^2} \right]^{\frac{1}{n+1}}; \quad (30)$$

The radius of a spinning BH is smaller than the radius of a Schwarzschild BH of equal mass.

The  $D$ -dimensional Schwarzschild BH has different mechanical and thermodynamical properties from its four-dimensional analogue. Agyres, Dimopoulos and March-Russell<sup>17</sup> have discussed the properties of spherically symmetric black holes in higher-dimensional spacetimes. The Hawking temperature and the entropy of a  $(n+4)$ -dimensional BH are

$$T_H = \frac{n+1}{4 r_s}; \quad S = \frac{(n+1)M_{BH}}{(n+2)T_H}; \quad (31)$$

respectively. Neglecting factors of order  $O(1)$ , the lifetime of a BH with mass  $M_{BH}$  is

$$\frac{1}{M_{\text{pl}}} \frac{M_{BH}^{\frac{n+3}{n+1}}}{M_{\text{pl}}^{\frac{n+3}{n+1}}}; \quad (32)$$

Higher-dimensional BHs are colder, longer-lived and with a greater radius than four-dimensional BHs of equal mass. Thus BH production is easier in higher dimensions.

At super-Planckian energies we expect formation of either Schwarzschild or Kerr BHs. The classical description is valid if the entropy of the process is sufficiently large, i.e., the fluctuations of the number of (micro) canonical degrees of freedom are small. BHs with mass equal to a few Planck masses usually satisfy this condition. For example, in  $D = 10$  dimensions the entropy of a Schwarzschild BH with mass equal to 5 (10) times the fundamental scale is  $S \approx 8$  (17). The lifetime of these BHs is larger than the inverse of their mass. From Eq. (32) it follows that  $M_{\text{BH}} \approx (M_{\text{Pl}})^{2(n+2)/(n+1)}$ . For a ten-dimensional BH with mass  $M_{\text{BH}} \approx 5$  (10)  $M_{\text{Pl}}$  we have  $M_{\text{BH}} \approx 40$  (190)  $M_{\text{Pl}}$ . The BHs formed in super-Planckian collisions can be thought as long-lived intermediate states, i.e., resonances.

### 3.2. BH Production

The physics of BH formation in hard collisions has been first described in detail by Banks and Fischler<sup>25</sup> and later by Giddings and Thomas in Ref.<sup>27</sup>. Super-Planckian particle collision processes are dominated by BH formation in the s-channel. The initial state is described by two incoming Aichelburg-Sexl shock waves with impact parameter  $b$ . If the impact parameter is smaller than the Schwarzschild radius associated with the CM energy of the incident particles, an event horizon forms. At super-Planckian energies the process of BH formation is semiclassical. Therefore, the cross-section is approximated by the geometrical cross section of an absorptive black disk with radius  $r_s$ :

$$\sigma_{ij \rightarrow \text{BH}}(s; n) = F(s) r_s^2; \quad (33)$$

where  $\sqrt{s}$  is the CM energy of the colliding particles and  $F(s)$  is a dimensionless form factor of order one. Using Eqs. (28) and (29) the cross section for a non-rotating BH is

$$\sigma_{ij \rightarrow \text{BH}}(s; n) = F(s) \frac{1}{s_?} (n)^2 \frac{s}{s_?} \frac{1}{n+1}; \quad (34)$$

where  $s_? = M_{\text{Pl}}^2$ . The form factor  $F(s)$  reflects the theoretical uncertainties in the dynamics of the process, such as the amount of initial CM energy that goes into the BH, the distribution of BH masses as function of the energy, and corrections to the geometrical black disk cross section.  $F(s)$  is usually chosen equal to one. Possible corrections to the cross section (34) have been described by Anchordoqui et al. in Ref.<sup>43</sup>. We summarize them here:

- a) Mass ejection corrections. Numerical simulations suggest that, at least in four-dimensions and in head-on collisions, the mass of the BH is less than the CM energy of the incoming particles<sup>88;89;90</sup>, i.e., the scattering is not completely inelastic. This result seems to suggest that  $F(s) < 1$ .<sup>i</sup>

<sup>i</sup>See also Ref.<sup>91</sup>.



Fig. 2. Schematic illustration of BH formation by super-Planckian scattering of two incident particles  $i$  and  $j$  with impact parameter  $b$ . The event horizon forms before the particles come in causal contact.

- b) Angular momentum corrections. Equation (30) suggests that BHs with nonvanishing angular momentum have smaller cross sections. The correction factor has been estimated by Anchordoqui et al.<sup>43</sup>. They found that angular momentum corrections lead typically to a reduction of the cross-section of about 40%.<sup>j</sup>
- c) Sub-relativistic limit. A naive argument based on the non-relativistic limit of a two-BH scattering suggests that the geometrical cross section can be enhanced by a factor  $< 400\%$ .
- d) Gravitational infall corrections. Solodukhin<sup>93</sup> used the classical cross section for photon capture of a BH to estimate the cross section of BH formation. With this definition, the cross section is enhanced by a factor ranging from 400% ( $n = 1$ ) to 87% ( $n = 7$ ).
- e) Voloshin suppression. The most controversial correction to the cross section (34) has been proposed by Voloshin<sup>94,95</sup>. Voloshin's claim is that BH creation must be described by an instanton. Thus the black disk cross section (34) has to be multiplied by a suppression factor proportional to  $e^{-S_E}$ , where  $S_E$  is the BH Euclidean action. Although the controversy has not yet been completely solved, numerical simulations in head-on collisions<sup>k</sup> seem to contradict Voloshin's result.

In the following sections we will set  $F(s) = 1$ . However, as a reminder of a possible uncertainty of order  $O(1)$ , we will also replace the equal sign with  $\sim$ .

The Schwarzschild radius of a BH with mass  $M_{BH} \sim M_p$  is of order of the fundamental Planck length. Therefore, in a hadronic collision, the cross section (34) must be interpreted at the parton level. For a proton-proton (pp) and a neutrino-proton ( $\nu p$ ) collision the total cross sections are

$$\sigma_{pp \rightarrow BH}(x_m; n) \sim \int_{x_m}^1 \int_{x_m}^1 dx \frac{dy}{y} f_i(y; Q) f_j(x=y; Q) \sigma_{ij \rightarrow BH}(xs; n); \quad (35)$$

and

$$\sigma_{\nu p \rightarrow BH}(x_m; n) \sim \int_{x_m}^1 dx f_i(x; Q) \sigma_{ij \rightarrow BH}(xs; n); \quad (36)$$

<sup>j</sup>See also Ref.<sup>92</sup>.

<sup>k</sup>See a).

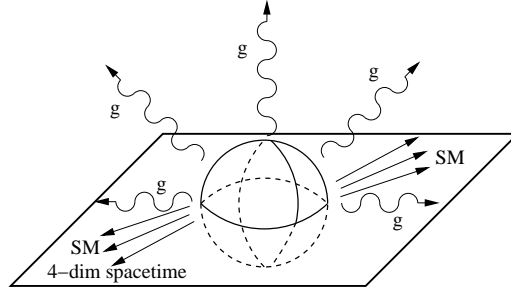


Fig. 3. Schwarzschild stage of BH evaporation. The BH emits brane and bulk modes. The former are SM fields that can be observed. The gravitons  $g$  are emitted in the bulk and cannot be observed.

respectively. Here,  $\overline{\sigma_{SM}} = M_{BH, min}^{-2}$  for  $M_{BH, min} \geq M_{\text{min}}$  is the minimal BH mass for which the semiclassical cross section (34) is valid,  $f_i$  are the Parton Distribution Functions (PDFs), and  $Q$  is the momentum transfer.<sup>1</sup> The sum over partons in Eq. (35) and Eq. (36) leads to a big enhancement of the BH cross section w.r.t. cross section of perturbative SM processes.

### 3.3. BH Decay and Experimental Signatures

A lot of efforts have been devoted to the study of the experimental signatures of BH production. After its formation, a BH evaporates semiclassically in a time  $t \sim 10^{-25}$  sec. by emitting Hawking radiation<sup>26, m</sup>. The decay phase is divided in three stages. In the first stage the BH sheds the hair associated with multipole momenta by emitting gauge radiation (SM fields on the brane and gravitons in the bulk). In the second stage the BH loses angular momentum, before evaporating by emission of thermal Hawking radiation with temperature  $T_H$  (last stage). The Hawking evaporation ends when the mass of the BH approaches  $M_{\text{min}}$ . At this point the semiclassical description breaks down (see Table 4) and the BH is believed to decay completely by emitting a few quanta with energy of order of  $M_{\text{min}}$ .

Emparan et al.<sup>98</sup> have found that BHs decay by emitting mainly on the brane. This can be qualitatively understood as follows. Since the wavelength of the thermal spectrum is much larger than the size of the BH, the latter evaporates in the  $s$ -channel. Therefore, BHs decay equally in all modes. Since the SM fields only propagate on the brane, the number of states emitted on the brane is greater than the number of states emitted in the bulk. Excluding the Higgs boson(s), the ratio of the degrees of freedom of SM gauge bosons, quarks and leptons on a brane with minimal thickness is 29:72:18. This leads to a final hadronic to leptonic

<sup>1</sup>In numerical calculations throughout the paper we will use the CTEQ6 PDFs<sup>96</sup>.

<sup>m</sup>The lifetime of a BH in the microcanonical picture is longer than in the canonical picture. In particular, in the RS model the evaporation process of BHs could be frozen at the fundamental Planck scale (see Ref.<sup>97</sup>).

activity roughly 5:1 and a ratio of hadronic to photonic activity of about 100:1. The experimental signatures of BH decay have been summarized in Ref. <sup>27</sup>. The most important are:

- a) Hadronic to leptonic activity of roughly 5:1;<sup>n</sup>
- b) High multiplicity;
- c) High sphericity;<sup>o</sup>
- d) Visible transverse energy of order 30% of the total energy;
- e) Emission of a few hard visible quanta at the end of the evaporation phase;
- f) Suppression of hard perturbative scattering processes.

The events that can potentially lead to BH production are essentially high-energy scattering in particle colliders and UHECR. The next generation of particle colliders are expected to reach energies above 10 TeV. LHC <sup>33</sup> (in construction at CERN) and VLHC <sup>34</sup> are planned to reach a CM energy of 14 and 100 TeV with a luminosity  $\mathcal{L}$  of  $300 \text{ fb}^{-1} \text{ yr}^{-1}$ , respectively. Therefore, if the fundamental Planck scale is of order of few TeV, LHC and VLHC would copiously produce BHs. A number of authors have studied the production rates of BH at LHC and other particle colliders <sup>100;101;29</sup>. In Fig. 4 we present the total cross sections for events at LHC. For this particular choice of parameters the cross section is in the range  $10^3 \text{ pb}$  (high thresholds) to  $10^2 \text{ pb}$  (low thresholds). With a luminosity of  $3 \times 10^6 \text{ pb}^{-1} \text{ yr}^{-1}$ , LHC might create BHs at a rate of one event per second! Rizzo has calculated the cross section and the production rate of BH formation at LHC when the Voloshin suppression is active. Though greatly reduced, the cross section is still sufficiently large to allow observation of BH formation at LHC <sup>100;101</sup>. For instance, for a minimum BH mass of 5 TeV and  $M_{\text{pl}} = 1 \text{ TeV}$ , the integrated cross section (35) is in the .1 to 1 pb range. Finally, other interesting possible signatures of BH formation at particle collider have been discussed by Uehara <sup>30;31</sup> and Anchordoqui and Goldberg <sup>32</sup>.

BH production by cosmic rays has also been recently investigated by a number of authors <sup>36;42;43;40;41;38</sup>. Cosmogenic neutrinos <sup>102</sup> with energies above the Greisen-Zatsepin-Kuz'min (GZK) cutoff <sup>103;104</sup> are expected to create BHs in the terrestrial atmosphere. The thermal decay of the BHs produces air showers which could be observed. The cross sections of these events are two or more orders of magnitude larger than the cross sections of SM processes (see Fig. 5). Therefore, BHs are created uniformly at all atmospheric depths with the most promising signal given by quasi-horizontal showers which maximize the likelihood of interaction. This allows BH events to be distinguished from other SM events.

<sup>n</sup>Recently, Han et al. <sup>99</sup> have investigated BH evaporation on a FB (see Sect. 2.3.2). They find that the hadronic to leptonic to photonic activity is 113:8:1.

<sup>o</sup>This is valid if the BH is at rest in the CM frame, i.e., for the completely inelastic collision  $ij \rightarrow \text{BH}$ . If SM particles are present in the final state, i.e., the process is  $ij \rightarrow \text{BH} + k$ , the BH is boosted and the decay is not spherical <sup>54</sup>.

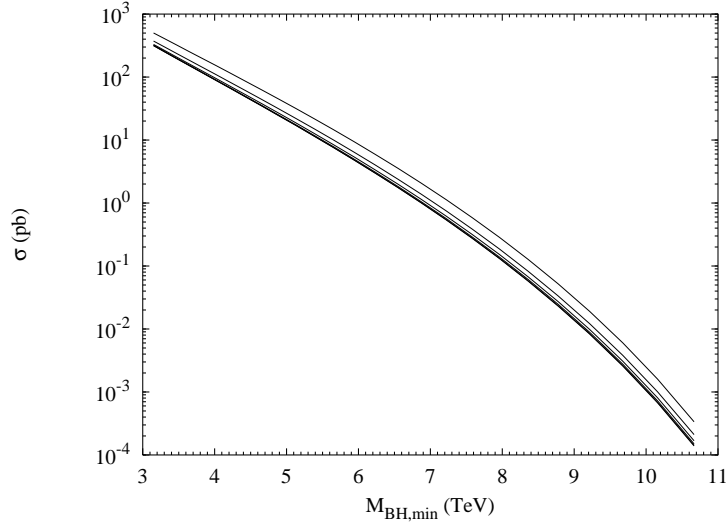


Fig. 4. Total cross sections (pb) for BH formation ( $n = 2:::7$  from above) by proton-proton scattering at LHC (CM energy = 14 TeV). We have assumed  $M_{\text{pl}} = 1$  TeV and a threshold for BH formation  $M_{\text{BH,min}} = 3M_{\text{pl}}$ .

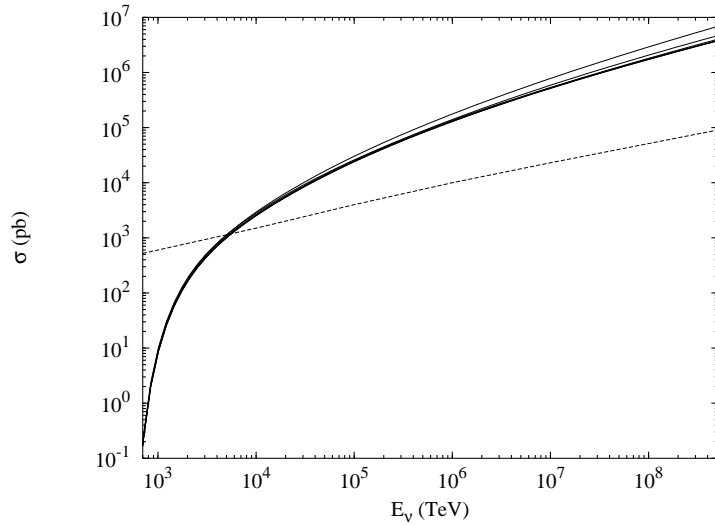


Fig. 5. Total cross sections (pb) of BH production by UHECR (neutrinos of energy  $E_{\nu}$ ,  $n = 2:::7$  from above). The dashed curve is for the SM process. We have assumed  $M_{\text{pl}} = 1$  TeV =  $M_{\text{BH,min}}$ .

The current non-observation of BH events at particle colliders and of BH-induced air showers in cosmic ray experiments sets lower bounds on the fundamental Planck scale. Bleicher et al.<sup>105;106</sup> find  $M_{\text{pl}} > 1.4$  TeV from Tevatron data

(CM energy = 1.8 TeV). The lower bounds on the fundamental Planck scale derived from UHECR experiments are given in Refs.<sup>36;42;43</sup>. Data from the Akeno Giant Air Shower Array<sup>107</sup> (AGASA) set a lower bound of  $M_{\text{pl}} = 1.65 \times 10^{16}$  GeV for  $n = 4$  and  $M_{\text{pl}} = 1.55 \times 10^{16}$  GeV for  $n = 7$ . Future UHECR experiments such as Auger<sup>108</sup> will either set more stringent limits on  $M_{\text{pl}}$  or detect several BH events per year.

#### 4. Brane Factories

Super-Planckian particle collisions may create extended objects other than BHs. The simplest extended object in  $D$  dimensions is described by the metric

$$ds^2 = g_{ab}(x)dx^a dx^b = -dt^2 + f(y) \sum_{m=1}^p dy^m dy^m + \sum_{n=1}^{D-p} dz^n dz^n; \quad (37)$$

where  $t = 0; \dots; D-p-1, m; n = D-p; \dots; D-1$ , and  $g$  is a pseudo-Riemannian metric in  $D-p$  dimensions. Equation (37) includes as special cases the  $p$ -brane metrics mentioned in the Introduction. The (Poincaré) $_{p+1}$   $SO(N-p-1)$  symmetry is obtained by setting  $g_{00} = -f(y) = -f(r)$ ,  $g_{0i} = 0$ , and  $g_{ij} = g(r) \delta_{ij}$ , where  $r = (\sum_{i=1}^p y_i^2)^{1/2}$  and  $i; j = 1; \dots; D-p-1$ . In "Schwarzschild-like" coordinates the  $p$ -brane metric is

$$ds^2 = A(r) (-dt^2 + dz_1^2) + B(r) dr^2 + r^2 C(r) d\Omega_{q-1}^2; \quad (38)$$

$p$ -branes arise as solutions of low-energy effective gravity and have been widely studied in the literature. In the next two sections we will briefly review brane solutions in Einstein-Maxwell gravity and low-energy effective STs.

##### 4.1. Einsteinian Branes

The  $p$ -brane solutions of Einstein-Maxwell-dilaton gravity have been discussed by Gregory<sup>47</sup>. The general uncharged non-spinning Einsteinian brane solution of  $(n+4)$ -dimensional Einstein gravity is<sup>48</sup>

$$ds^2 = -R dt^2 + R^{\frac{p}{p+q}} dz_1^2 + R^{\frac{1}{q-1}} [1 + \frac{p}{p+q}] R^{-1} dr^2 + r^2 d\Omega_{q-1}^2; \quad (39)$$

where

$$R = 1 - \frac{r_p^{q-1}}{r}; \quad (40)$$

and  $r_p$  and  $q$  are two parameters related by

$$j = \frac{p}{q(p+q)} + \frac{p}{q(p+q)} - 1 = \frac{1}{p+q} \quad (41)$$

The line element is singular on the hypersurface  $r = r_p$ . The nature of the singularity depends on the value of the modulus  $j$ . Setting

$$R(r) = 1 - \frac{r_p^{q-1}}{r} = 1 - \frac{r_p^{q-1}}{r} R^{-1}(r); \quad (42)$$

the metric is cast in the form

$$ds^2 = R^2 dt^2 + R^{\frac{2}{p+q}} dz_i^2 + R^{\frac{2}{q-1}} [1 + (\frac{r}{R})^{\frac{2}{p+q}}] R^{-1} dr^2 + r^2 d\Omega_q^2 ; \quad (43)$$

The metric (43) covers only the exterior part of the p-brane spacetime. Equation (43) is obtained from Eq. (39) with the substitution  $r \rightarrow R \frac{r}{R}$  and  $\frac{r}{R} \rightarrow \frac{r}{R} \frac{R}{r}$ . In the following we will choose  $R = 1$  without loss of generality. The (boosted) p-brane solution is obtained by choosing  $\alpha = (p+q)^{-1}$ . The line element is

$$ds^2 = R^{\frac{2}{p+1}} ( dt^2 + dz_i^2 ) + R^{\frac{2-q}{q-1}} dr^2 + r^2 R^{\frac{1}{q-1}} d\Omega_q^2 ; \quad (44)$$

where

$$R = \frac{r}{p+q} ; \quad (45)$$

The spherically symmetric solution is recovered for  $p = 0$ ; in this case we have  $\alpha = 1$ , and Eq. (44) reduces to the  $(n+4)$ -dimensional Schwarzschild BH. Equation (44) describes an asymptotically flat spacetime. When  $p = 0$  (BH)  $r = r_p = r_s$  defines the Schwarzschild horizon. For  $p \neq 0$  the metric (44) possesses a non-conical <sup>109</sup> naked singularity at  $r = r_p$  which is the higher-dimensional analogue of a cosmic string singularity.  $r_p$  can be interpreted as the "physical radius" of the p-brane. The interpretation of the curvature singularity has been discussed in Ref. <sup>47</sup>. The metric (44) is interpreted as vacuum exterior solution to the p-brane, with the curvature singularity being smoothed out by the core of the p-brane.

The previous solutions can be generalized to include electromagnetic charge and dilaton field <sup>47</sup>. In the Einstein frame (4) the general black brane solution is <sup>51</sup> ( $a = 1=2$ )

$$ds^2 = R_+ R^{\frac{2}{p+1} (1 + \frac{qb^2}{2(q-1)})} dt^2 + R^{\frac{2}{p+1} (1 + \frac{qb^2}{2(q-1)})} dz_i^2 + R_+^{-1} R^{\frac{2}{q-1} (1 + \frac{2(q-1)}{qb^2})} dr^2 + r^2 R^{\frac{2}{q-1} (1 + \frac{2(q-1)}{qb^2})} d\Omega_q^2 ; \quad (46)$$

$$= e^{-\frac{2}{b} (1 + \frac{2(q-1)}{qb^2})} \ln R ; \quad (47)$$

where  $\phi$  is the dilaton field and

$$R = 1 - \frac{r}{r_+} ; \quad (48)$$

The boosted magnetically charged solution with EM field  $F_{[n]} = Q \omega_n$  has been given by Gregory in Ref. <sup>47</sup>.

$$ds^2 = e^{\frac{2(q-1)}{b(p+q)}} R_+^{\frac{2}{p+1}} R^{\frac{2}{p+1}} ( dt^2 + dz_i^2 ) + e^{\frac{2(p+1)}{b(p+q)}} R_+^{\frac{2}{q-1}} R^{\frac{2}{q-1}} dr^2 + e^{\frac{2(p+1)}{b(p+q)}} r^2 R_+^{\frac{1}{q-1}} R^{\frac{1}{q-1}} d\Omega_q^2 ; \quad (49)$$

$$= e^{-\frac{2}{b} (1 + \frac{2(q-1)}{qb^2})} \ln \left( 1 - \frac{r}{r_+} \right) ; \quad (50)$$

where

$$Q^2 = \frac{4(q-1)^2}{b^2} \left[ 1 + \frac{2^{-2}(q-1)}{qb^2} r^{2(q-1)} \left[ (1 - r_+^q)^{-1} r^{-q} \right] \right] \quad (51)$$

The electrically charged solution is obtained by a duality transformation<sup>47</sup>. A  $p$ -brane is always dual to a  $(D-p-4)$ -brane. If the spacetime dimension is even, self-dual branes with  $p = D-2$  and  $q = D-2$  exist. Self-dual branes are discussed in Ref.<sup>47</sup>. The extremal limit of Eqs. (47) and (49) is obtained by setting  $r_+ = r_-^p$ . The metric and the dilaton are

$$ds^2 = R^{\frac{2}{p+1} + \frac{qb^2}{2^{-2}(q-1)}} \left( dt^2 + dz_1^2 \right) + R^{\frac{2}{q-1} + q + 1 + \frac{2^{-2}(q-1)}{qb^2}} dr^2 + r^2 R^{\frac{2}{q-1} + 1 + \frac{2^{-2}(q-1)}{qb^2}} d\Omega_q^2; \quad (52)$$

$$= \frac{2}{b} \left[ 1 + \frac{2^{-2}(q-1)}{qb^2} \right] \ln R; \quad (53)$$

If we set  $b \rightarrow 0$  in Eq. (47) the dilaton field decouples. The general Einstein-Maxwell solution is

$$ds^2 = R_+ R^{\frac{1-p}{1+p}} dt^2 + R^{\frac{2}{1+p}} dz_1^2 + (R_+ R)^{-1} dr^2 + r^2 d\Omega_q^2 \quad (54)$$

The extremal Einstein-Maxwell brane is obtained by setting  $R_+ = R_- = R$ :

$$ds^2 = R^{\frac{2}{1+p}} \left( dt^2 + dz_1^2 \right) + R^{-2} dr^2 + r^2 d\Omega_q^2; \quad (55)$$

Setting  $p = 0$  in Eqs. (54) and (55) we recover the Reissner-Nordstrom solution.

#### 4.2. String and Supergravity Branes

The general solution of the previous section includes branes of SUPERGRAVITY theories. Let us see a few examples. Choosing

$$b = \frac{r}{\frac{2}{p+q}} (q-1) \quad (56)$$

in Eq. (49), and passing to the string frame

$$g_{ab}^s = \exp \left[ \frac{r}{\frac{2}{p+q}} \right] g_{ab}; \quad (57)$$

Eq. (49) and (50) read

$$ds^2 = R_+^{\frac{2}{p+1}} R^{\frac{2}{p+1}} \left( dt^2 + dz_1^2 \right) + e^{\frac{p}{\frac{2}{p+q}}} R_+^{\frac{1}{q-1}} R^{\frac{1}{q-1}} (R_+ R)^{-1} dr^2 + r^2 d\Omega_q^2; \quad (58)$$

$$= \frac{r}{\frac{2}{p+q}} \ln \left[ \frac{1 - R_+ R}{(1 - r_+^q)^{-1} r^{-q}} \right]; \quad (59)$$

<sup>47</sup>Note that the extremal limit of the generic black brane solution is a boosted brane.

The non-supersymmetric five-brane in ten dimensions is obtained by setting  $p = 5$  and  $q = 3$ :

$$ds^2 = \frac{R_+}{R} (dt^2 + dz_1^2) + e^2 R_+^{-1} R^{5-4} (R_+ R)^{-1} dr^2 + r^2 d\Omega_3^2 ; \quad (60)$$

The six-brane of ten-dimensional heterotic ST is obtained by choosing  $p = 6$  and  $q = 2$ :

$$ds^2 = \frac{R_+}{R} (dt^2 + dz_1^2) + e^4 \frac{R_+}{R} dr^2 + R_+ R r^2 d\Omega_2^2 ; \quad (61)$$

The electrically charged solution dual to the six-brane (61) is the zero-brane

$$ds^2 = R_+ R dt^2 + R_+^{-1} R^{5-7} dr^2 + r^2 R^{2-7} d\Omega_8^2 ; \quad (62)$$

Setting  $p = 5$  and  $q = 4$  in Eq. (55) we obtain the (extremal) solitonic/magnetic five-brane of 11-dimensional SUGRA<sup>51</sup>:

$$ds^2 = R^{1-3} (dt^2 + dz_1^2) + R^2 dr^2 + r^2 d\Omega_4^2 ; \quad (63)$$

The corresponding dual electric two-brane is<sup>51</sup>

$$ds^2 = R^{2-3} (dt^2 + dz_1^2) + R^2 dr^2 + r^2 d\Omega_7^2 ; \quad (64)$$

The magnetic five-brane (63) and the electric two-brane (64) saturate the Bogomol'nyi bound<sup>50</sup> (BPS solutions). Thus they leave some portion of supersymmetry unbroken. It can be shown<sup>51</sup> that Eqs. (63) and (64) preserve half of the rigid  $D = 11$  supersymmetry.

#### 4.3. p-brane Mass and Radius

The parameters  $r_p$  and  $r$  are related to the ADM<sup>110</sup> mass  $M_p$  and to the electric/magnetic charge  $Q$  of the brane. The general formula for the ADM mass of a p-brane has been derived by Lu<sup>111</sup>. Given a generic metric of the form

$$ds^2 = A(r)dt^2 + D(r)dz_1^2 + B(r)dr^2 + r^2 C(r)d\Omega_q^2 ; \quad (65)$$

the ADM mass of the brane is:

$$M_p = M_p^q v_p \frac{r_p^{\frac{q-1}{2}}}{8^{\frac{q+1}{2}}} r^q [q\ell_r C(r) + p\ell_r D(r)] + q r^{q-1} [B(r) - C(r)]_{r=r_p} ; \quad (66)$$

where  $v_p$  is the p-dimensional volume of the brane in fundamental Planck units. For instance, the ADM mass of the neutral Einsteinian p-brane (44) in  $n+4$  dimensions is

$$M_p = M_p^{n+2} v_p \frac{r_p^{p-n-1}}{(n;p)} ; \quad (67)$$

where

$$(n;p) = 8 \frac{n+3-p}{2} \frac{s}{(n+2)(n+2-p)} \# \frac{1}{n+1-p} ; \quad (68)$$

Inverting Eq. (68) we obtain the p-brane radius

$$r_p = \frac{1}{M_p} \left( \frac{M_p}{M_{\text{pl}}} \right)^{\frac{w}{n+1}} v_p \quad (69)$$

where  $w = [1 - p(n+1)]^{-1}$ . For  $p = 0$  (0-brane)  $w = 1$  and we recover Eqs. (28) and (29).

#### 4.4. Brane Formation in TeV Gravity

In analogy to the BH case, scattering of two partons with impact parameter  $b < r_p$  produces a p-brane which is described by a suitable localized energy density configuration and whose exterior geometry has metric (38). Assuming that the collision is completely inelastic, the cross section for the process depends on the brane tension. The geometrical cross section corresponding to the black absorptive disk of radius  $r_p$ <sup>52</sup> is:

$$\sigma_{ij \rightarrow \text{br}} = F(s) r_p^2 \quad (70)$$

Setting  $F(s) = 1$ <sup>9</sup>, the cross section (70) is given by

$$\sigma_{ij \rightarrow \text{br}}(s; p; n; v_p) = \frac{1}{s_2} G(n; p) v_p \frac{s}{s_2}^{\frac{1}{n+1}} \quad ; \quad (71)$$

where  $s = E_{ij}^2$  is the square of the CM energy of the two scattering partons, and  $s_2 = M_{\text{pl}}^2$ . The function  $G(n; p)$  depends on the model considered. For instance,

$$G_{\text{Ein}}(n; p) = (n; p)^2 = \frac{64(p+1) [(n+3-p)2]^{\frac{1}{n+1}}}{(2+n)(n-p+2)} \quad ; \quad (72)$$

for the Einsteinian brane and

$$G_{\text{el}}(n; p) = 2; \quad G_{\text{mag}}(n; p) = (2^p)^{2=3} \quad ; \quad (73)$$

for the electric and magnetic SUGRA branes, respectively.

Let us focus attention on the Einsteinian brane (44) and compare the cross section for p-brane production to the BH cross section (34). The ratio of p-brane and BH cross sections is

$$\frac{\sigma_{ij \rightarrow \text{br}}(s; n; p; v_p)}{\sigma_{ij \rightarrow \text{BH}}} = v_p \frac{s}{s_2}^{\frac{w}{n+1}} \frac{G_{\text{Ein}}(n; p)}{G_{\text{Ein}}(n; 0)} \quad ; \quad (74)$$

Since  $w > 1$  for any  $n - p > 0$ , becomes larger for higher energy. At fixed  $n$  and  $s$  the value of depends on the dimensionality of the brane and on the size of the extra dimensions. Let us consider the scenario with  $m$  extra dimensions compactified on the  $L$  scale and  $n - m$  dimensions compactified on the  $L^0$  scale (see Eq. (20)). The  $L$ -size dimensions can be identified with the small dimensions and

<sup>9</sup>See Sect. 3.2.

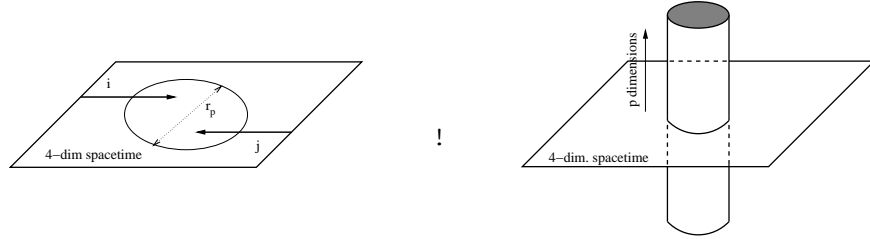


Fig. 6. Schematic illustration of brane formation by super-Planckian scattering of two incident particles with impact parameter  $b$ .

are compactified at about the Planck scale. If we assume that the  $p$ -brane wraps on  $r$   $L$ -size dimensions ( $r = m$ ) and on  $p - r$   $L^0$ -size dimensions, the  $p$ -brane volume  $V_p$  is

$$V_p = L^r L^{(p-r)} = L^{\frac{nr}{n-m} - \frac{mp}{n-m}} \frac{M_{Pl}^{\frac{2(p-r)}{n-m}}}{M_*} : \quad (75)$$

Substituting Eq. (75) in Eq. (74) we find

$$(s; n; m; p; r) = 1 \frac{M_{Pl}}{M_*} \frac{G_{E, in}(n; p)}{G_{E, in}(n; 0)} \frac{s}{s_*}^{\frac{w-1}{n+1}} ; \quad (76)$$

where

$$= \frac{2(nr - mp)}{(n-m)(n-p+1)} \ll 0 ; \quad = \frac{4(p-r)}{(n-m)(n-p+1)} \ll 0 : \quad (77)$$

In TeV scale gravity,  $M_{Pl} = M_* = 10^{16}$  ( $10^{16}$ ) for  $M_* = 100$  TeV (1 TeV). Since  $0 < (w-1) = (n+1) < 1$ , the  $p$ -brane cross section is suppressed w.r.t. spherically symmetric BH cross section by a factor  $\ll 10^4$  ( $\ll 10^{16}$ ). The largest cross section is obtained for  $p = r$ , i.e., when the  $p$ -brane is completely wrapped on the small-size dimensions:

$$(s; n; m; p = m) = 1 \frac{2p}{n-p+1} \frac{G_{E, in}(n; p)}{G_{E, in}(n; 0)} \frac{s}{s_*}^{\frac{w-1}{n+1}} : \quad (78)$$

Assuming  $L = L_*$  the  $p$ -brane formation process dominates the BH formation process. When the  $p$ -brane is wrapped on some of the large extra dimensions, the  $p$ -brane cross section is suppressed w.r.t. BH cross section. The ratio slightly increases with the dimension of the brane. Therefore, in a spacetime with  $m$  fundamental-scale extra dimensions and  $n - m$  large extra dimensions a  $m$ -brane is the most likely object to be created. The cross sections are dramatically enhanced

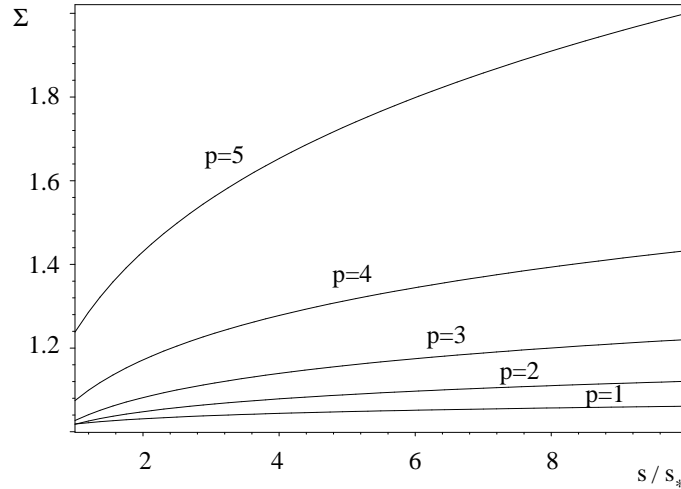


Fig. 7. Ratio between the cross section for the creation of  $p$ -branes ( $p \leq m$ ) completely wrapped on fundamental-size dimensions and a spherically symmetric BH in a 11-dimensional spacetime with  $m = 5$  fundamental-size extra dimensions  $L = M_{\text{pl}}^{-1} = (100 \text{ TeV})^{-1}$  and  $n - m = 2$  large extra dimensions of size  $L^0 = 10^2 (\text{TeV})^{-1} = L_{\text{pl}}$ .

if the  $p$ -brane wraps around dimensions which are smaller than the fundamental scale. In ST/T dualities and mirror symmetries usually set a lower bound on compactification dimensions in the weak coupling regime of order  $O(L_{\text{pl}})$ . However, it is not unreasonable to assume, for instance,  $L = L_{\text{pl}}/2$  or  $L = L_{\text{pl}}/4$ .<sup>†</sup> In this case the cross section may be enhanced by one or even two orders of magnitude.

Let us consider the 11-dimensional spacetime as a concrete example. Assume  $m = 5$  fundamental-scale extra dimensions  $L = M_{\text{pl}}^{-1} = (100 \text{ TeV})^{-1}$  and two large extra dimensions  $L = 10^2 (\text{TeV})^{-1}$ . At  $s = 10s_*$  the cross sections for the formation of a 5-brane and a 4-brane completely wrapped on the fundamental-size dimensions are enhanced by a factor 2 and 3=2 w.r.t. cross section for creation of a spherically symmetric BH, respectively. (See Fig. 7). If the 5-brane wraps on four extra dimensions with fundamental-scale size and on one large extra dimension, ( $s = 10s_*$ ) is suppressed by a factor  $10^8$ . Assuming  $L = L_{\text{pl}}/2$  ( $L = L_{\text{pl}}/4$ ) the cross section for the creation of 5-branes in a 11-dimensional spacetime is enhanced

<sup>†</sup>It should be stressed that  $L_{\text{pl}}$  denotes the fundamental scale rather than the minimum distance. Therefore, compactifications with size (not too) smaller than  $L_{\text{pl}}$  are possible in principle. Analogy with elementary quantum mechanics is illuminating.  $h$  denotes the scale of quantum processes in quantum mechanics. However, processes with scale smaller than  $h$  are possible; a harmonic oscillator satisfies  $x = p = h/2$ . In TeV-gravity  $L_{\text{pl}}$  denotes the scale of quantum gravity processes. By analogy, compactifications with size  $L = L_{\text{pl}}/2$  seem not to be unreasonable.

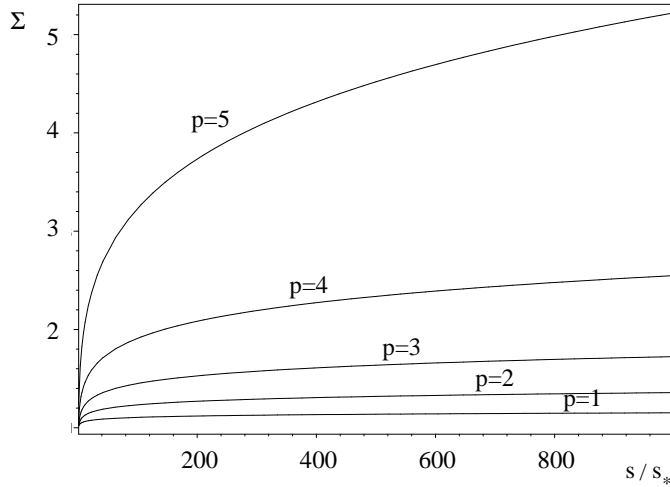


Fig. 8. Ratio between the cross section for the creation of  $p$ -branes ( $p \leq m$ ) completely wrapped on fundamental-size dimensions and a spherically symmetric black hole in a spacetime with  $m = 5$  fundamental-size extra dimensions  $L = M_{\text{pl}}^{-1} = (10 \text{ TeV})^{-1}$  and  $n - m = 2$  large extra dimensions of size  $L^0 = 10^4 (\text{TeV})^{-1} = 2 \cdot 10^{-10} \text{ cm}$ . If the fundamental-size extra dimensions have size  $L = L_{\text{pl}} = 4$  the cross sections are enhanced by a factor 100, 16, 5, 2, 3/2 for  $p = 5, 4, 3, 2$  and 1, respectively.

by a factor 10 (100).

Finally, let us consider symmetric compactifications. The ratio is

$$\frac{M_{\text{pl}}}{M_{\text{?}}} = \frac{\frac{4\omega p}{n(n+1)} G_{\text{Ein}}(n;p)}{G_{\text{Ein}}(n;0)} \frac{s}{s_{\text{?}}}^{\frac{\omega-1}{n+1}} \quad (79)$$

In this case the cross section for  $p$ -brane formation is subdominant to the cross section for BH formation. This result is understood qualitatively as follows. If all the extra dimensions have (large) identical characteristic size, the spacetime appears isotropic to the  $p$ -brane and a spherically symmetric object is likely to form (see discussion in Sect. 3.1). Conversely, when the compactification is asymmetric non-spherically symmetric objects are more likely to be created. In an asymmetric model with  $m$  small extra dimensions the most likely  $p$ -brane to form is that with the highest symmetry compatible with spacetime symmetries, i.e., a  $m$ -brane.

#### 4.5. Brane Production on Fat Branes

Recently, Cheung and Chou<sup>112</sup> have investigated Einsteinian  $p$ -brane formation in FB and UED models (see Sect. 2.3.2). In these models the production rate of  $p$ -branes relative to BHs can be enhanced by a much larger factor than in the ADD

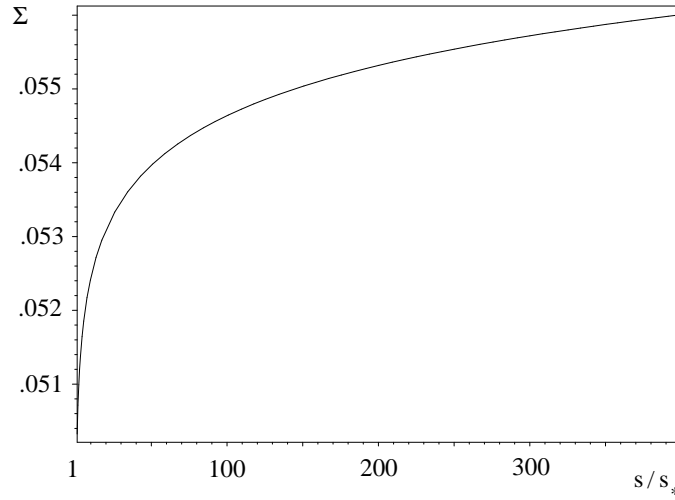


Fig. 9. Ratio between the cross section for the creation of a string ( $p = 1$ ) and a spherically symmetric BH in a 11-dimensional spacetime with symmetric compactification ( $L_p = 1 \text{ TeV}^{-1}$ ). The cross section for string formation is suppressed w.r.t. the cross section for BH formation by a factor  $\alpha = 20$ .

scenario. If the SM particles propagate in some of the extra dimensions, the cross section for producing a BH or a p-brane must scale as  $r_p^{k+2}$ :

$$\sigma_{ij}^{(k)} = F_k(s) r_p^{2+k}; \tag{80}$$

where  $k = n - 2$  is the number of extra dimensions in which the SM particles can propagate in addition to the four macroscopic ones.<sup>5</sup> Setting  $F_k(s) = 1$  and assuming  $L = L_p$ , the ratio of Einsteinian p-brane and BH cross sections is given by

$$\sigma_k(s; n; m; p; r) = \frac{\sigma_{ij}^{(k)} \text{ br}}{\sigma_{ij}^{(k)} \text{ BH}} = \frac{M_{Pl}^k}{M_*^k} \frac{G_{E \text{ in}}(n; p)}{G_{E \text{ in}}(n; 0)} \frac{s^{k+2+1}}{s_*^k} \frac{1}{n+1} (k=2+1); \tag{81}$$

where

$$k = \frac{2(2+k)(p-r)}{(n-m)(n-p+1)} \geq 0; \tag{82}$$

<sup>5</sup>At least two of the extra dimensions must be large to satisfy experimental constraints. Therefore the SM particles can propagate in  $n - 2$  extra dimensions at the most.

Equation (81) reduces to Eq. (76) for  $k = 0$ . For  $p$ -branes completely wrapped on the small extra dimensions ( $p = r$ ) Eq. (81) is

$$\frac{G_{\text{E in}}(n;p)}{G_{\text{E in}}(n;0)} \stackrel{k=2+1}{=} \frac{s}{s_?} \frac{w}{n+1}^{(k=2+1)} \quad ; \quad (83)$$

The largest ratio is obtained for  $k = p = m$ , i.e. when the SM particles propagate in all small extra dimensions and the dimension of the brane is equal to the number of small extra dimensions. Cheung and Chou have computed the ratio (83) for various values of  $n$  and  $p$  when  $k = p = m$ . The highest ratio is obtained for a 4-brane in a 11-dimensional spacetime (105). Therefore, in the FB or UED models the ratio of  $p$ -brane production to BH production can be as large as 100 without requiring compactification radii smaller than the fundamental scale. The ADD model with small extra dimensions  $L \ll L_p$  gives at most a ratio of order  $O(1)$ .

#### 4.6. Brane Decay and Thermodynamics

In contrast to BHs, the fate of  $p$ -branes depends strongly on the model. Branes are extended objects endowed with tension. Therefore, they are unstable unless some extra mechanism intervenes to stabilize them. A brane with horizon and non-vanishing entropy evaporates by emitting thermal Hawking radiation<sup>26</sup>. For instance, SUGRA branes of Sect. 4.2 evaporate by Hawking radiation, provided that the Bogomol'nyi bound is not saturated<sup>51;113</sup>. The thermodynamics of generic branes has been studied by Du et al. in Ref.<sup>50</sup>. However, a thorough investigation of brane evaporation in the TeV scenario is still missing.

The Hawking evaporation process does not occur for  $p$ -branes without horizon. Although the decay process of singular branes is not understood, string field theory arguments<sup>114;115;116;117;118;119;120</sup> and analogy to cosmic strings<sup>121;122;123</sup> provide some clue about brane decay. String field theory suggest that a higher-dimensional brane can be seen as a lump of lower-dimensional branes. The tension of the brane causes the latter to decay in lower dimensional branes, and eventually to evaporate in gauge radiation. A bosonic non-supersymmetric brane can be considered as an intermediate state in the scattering process. Pursuing further the analogy with particle physics, BHs can be regarded as metastable particles and branes their resonances.<sup>t</sup>

The Einsteinian uncharged  $p$ -brane (44) does not emit Hawking radiation during the earlier stages of the decay because of the singularity at  $r = r_p$ . However, the brane eventually decays in 0-branes and evaporate in a time of order  $M_p^{-1}$  by emitting "visible", possibly thermal, brane and bulk quanta. Though the intermediate states of the decay of a singular brane are highly dependent on the details of the theory considered, we do not expect significant qualitative differences as far

<sup>t</sup>The author is grateful to Angela O'linto for this remark.

as the final evaporation stage is concerned. It has also been conjectured that singularities could explode in a sudden burst instead of evaporating via the Hawking process<sup>124,97</sup>. However, no information about decay products nor estimate of the lifetime of the singularity are currently available. In either scenario (dimensional cascade followed by Hawking evaporation vs. naked singularity explosion) there is no reason to believe that brane decay does not lead to production of visible particles.

#### 4.7. Branes in the Randall-Sundrum Model

Brane production can be easily accommodated in the RS scenario<sup>125</sup>. The procedure follows closely that of Chamblin et al. for the black string in AdS<sup>126</sup>. In conformal coordinates the  $(p+1)$ -dimensional RS metric (21) is

$$ds^2 = \frac{r^2}{(r+z_0)^2} (dx^2 + dz^2); \quad (84)$$

where  $r$  is the AdS radius and the (single) brane is located at  $z = z_0$ . Motivated by ST/M-theory, in the following we consider a generalized  $D$ -dimensional RS model with  $D = 5$ . One of the  $n$  extra dimensions is large and warped and provides the solution to the hierarchy problem. The remaining  $n-1$  extra dimensions are flat and are of order of the fundamental Planck scale. The  $D$ -dimensional RS metric satisfies the Einstein equations

$$R_{ab} = \frac{D-1}{2} g_{ab} = -\Lambda g_{ab}; \quad (85)$$

If we replace the  $(D-1)$ -dimensional Minkowski metric in Eq. (84) with any Ricci flat metric, the Einstein equations (85) are still satisfied. Therefore, we can substitute Eq. (44) in Eq. (84) and obtain

$$ds^2 = \frac{r^2}{(r+z_0)^2} (ds_{br}^2 + dz^2); \quad (86)$$

where  $ds_{br}^2$  is the metric (44). Equation (86) describes a  $p$ -dimensional brane ( $p = D-5$ ) propagating on the  $(D-1)$ -dimensional wall located at  $z = z_0$ . In the original  $(p+1)$ -dimensional RS model the metric (86) is

$$ds^2 = \frac{r^2}{(r+z_0)^2} (R(r) dt^2 + R(r)^{-1} dr^2 + r^2 d\Omega_p^2 + dz^2); \quad (87)$$

Equation (87) describes a four-dimensional spherically symmetric BH propagating on the wall at  $z = z_0$ <sup>u</sup>. In eleven dimensions the metric (86) reads

$$ds^2 = \frac{r^2}{(r+z_0)^2} (R^{p+1} (dt^2 + dz_1^2) + R^{\frac{1}{q-1}} R^{-1} dr^2 + r^2 d\Omega_p^2 + dz^2); \quad (88)$$

where  $q = [(1-p)(p+1)]^{1/2}$  and  $p \geq 6$ .

<sup>u</sup> Alternatively, a black string propagating in the full  $(p+1)$ -dimensional AdS spacetime.

The cross section of brane production in the RS model depends on the AdS radius and on the location of the background brane  $z_0$ . Since only the warped dimension is large, the volume of a brane has Planck size. In the warped model we expect larger cross sections compared to the ADD scenario: the maximal dimension of the brane is  $p = D - 5$  in the former, while experimental constraints limit it to  $p \leq 6$  in the latter. A more complete investigation of brane production in RS scenario is currently in progress<sup>125</sup>. The phenomenology of RS BHs has been recently investigated in Ref.<sup>44</sup>

### 5. Brane formation at Particle Colliders

Like BHs, p-brane formation could be observed at particle colliders. The brane cross sections for proton-proton collisions and the brane production rates at LHC have been computed by Ahn and the author in Ref.<sup>53</sup> and independently by Cheung<sup>54</sup>. LHC with a proton-proton CM energy of 14 TeV will likely offer the first opportunity to observe brane formation. The total cross-section for a proton-proton event is given by Eq. (35) where  $\sigma_{ij \rightarrow \text{BH}} = \sigma_{ij \rightarrow \text{br}}$ :

$$\sigma_{pp \rightarrow \text{br}}(x_m; n; p; v_p) = \sum_{ij} \int_{x_m}^{z_1} dx \int_{x}^{z_1} \frac{dy}{Y} f_i(y; Q) f_j(x=y; Q) \sigma_{ij \rightarrow \text{br}}(xs; n; p; v_p); \quad (89)$$

The cross sections for production of Einsteinian branes at LHC are plotted in Fig 10. Assuming a fundamental Planck scale of  $M_* = 2$  TeV and  $D = 10$  dimensions, the cross sections are in the range  $10^{-4} - 10^3$  pb and increase for increasing brane dimension as expected. Therefore, the production rate of higher-dimensional branes is higher than production rate of spherically symmetric BHs. For a minimum brane mass of  $M_{\text{min}} = 3$  TeV, the cross section for a one- and a two-Einsteinian brane is  $\sigma_5 = 250$  pb and  $\sigma_2 = 90$  pb, respectively. Therefore, with a LHC luminosity  $\mathcal{L} = 3 \times 10^{34} \text{ pb}^{-1} \text{ yr}^{-1}$  we expect a one-brane event and a two-brane event approximately every .5 and 1 second.

The production of branes at particle colliders – if observed – would allow the investigation of the structure of the extra dimensions. Brane cross sections are very sensitive to the size of the brane, which is related to the size of the compactified extra dimensions around which the brane wraps. Since  $v_p$  is constant w.r.t. the sum on partons, the total cross section is enhanced if the length of the extra dimensions is sub-Planckian. For instance, the cross section of a one-brane wrapped on extra dimensions with size 1/2 of the fundamental scale is enhanced by a factor  $\sim 10$ .

If supersymmetry is unbroken and SUGRA describes the physics at energies above the TeV scale, high-energy particle scattering at particle collider could produce charged SUGRA branes (see Sect. 4.2). In order to produce SUGRA branes the collision must be either of the two processes

$$\begin{aligned} p^+ + p^+ &\rightarrow \text{brane} + X^q; \\ p^+ + p^+ &\rightarrow \text{brane} + \text{antibrane}; \end{aligned}$$

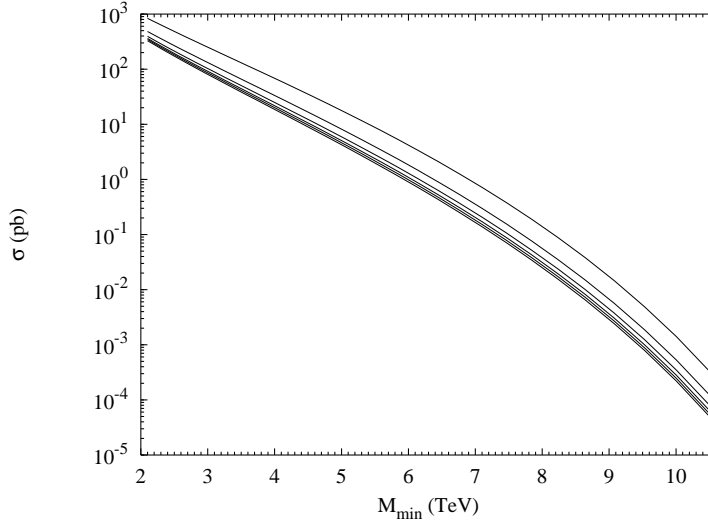


Fig. 10. Cross sections (pb) for the formation of branes more massive than  $M_{\min}$  (TeV) at LHC ( $D = 10$ ,  $p = 0 :: 4$  from below). The volume of the branes is assumed to be equal to one in fundamental Planck units ( $M_p = 2$  TeV).

where  $X^q$  denotes a set of particles with total charge equal to  $2e^+$  minus the brane charge. The cross sections for production of SUGRA branes are comparable to those of Einsteinian branes. (See, e.g., Fig. 11).

The experimental signatures depend on the decay process. If the brane possesses a horizon or decays into lower-dimensional branes, we expect an observed hadronic to leptonic activity of roughly 5:1, high multiplicity and emission of a few hard visible quanta at the end of the process. However, if the brane explodes in a sudden burst, or a stable SUGRA brane forms, the experimental signatures could be drastically different. In particular, an extremal brane would be detected either as missing energy or as a stable charged heavy particle. A comprehensive study of the experimental signatures of brane production in particle colliders is currently missing.

## 6. Brane Production and High Energy Cosmic Rays

In the TeV scenario UHECR can create p-branes. Unlike BHs (see Sect. 3.3) the production and the subsequent decay of p-branes in the terrestrial atmosphere could lead to formation of showers that might be detected by cosmic ray experiments<sup>35</sup>. The best candidate for brane formation are cosmogenic neutrinos<sup>102</sup>. The total cross section for neutral Einsteinian brane production was first computed in Ref.<sup>55</sup> and is obtained from Eq. (36) by substituting  $\sigma_{ij}^{\text{BH}}$  with  $\sigma_{ji}^{\text{br}}$ :

$$\sigma_{p\text{-br}}(x_m; n; p; v_p) = \sum_i \int_{x_m}^1 dx f_i(x; Q) \sigma_{ij}^{\text{br}}(xs; n; p; v_p); \quad (90)$$

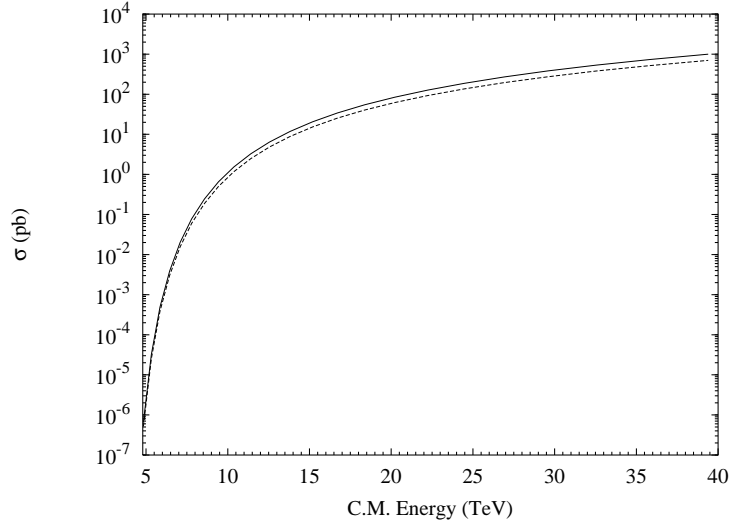


Fig. 11. Cross sections for creation of magnetic (solid curve) and electric (dashed curve) 11-dimensional SUGRA branes (Eqs. (63) and (64)) by proton-proton scattering with  $M_{\text{pl}} = 2 \text{ TeV}$ , minimum mass  $M_{\text{min}} = 2M_{\text{pl}}$ , and unit volume. The cross sections for the corresponding Einsteinian two- and five-brane are enhanced by a factor of  $\sqrt{2}$  and  $\sqrt{2/7}$ , respectively.

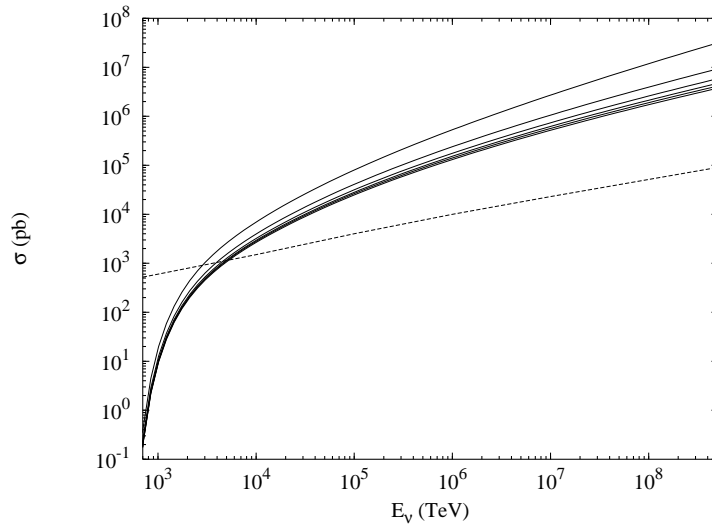


Fig. 12. Cross sections for creation of neutral Einsteinian branes by UHECR scattering with  $M_{\text{pl}} = M_{\text{min}} = 1 \text{ TeV}$ , unit volume, and  $n = 6$  ( $p = 0 :: 5$  from below). The dashed curve is for the SM process.

As usual, the cross section is enhanced if the small extra dimensions are compactified below the fundamental scale. The total cross section for a neutrino with

energy  $\sim 10^6$  TeV might reach the 100 mb range, a value which is comparable to SM nucleon-nucleon cross section at these energies. This fact led Jain et al.<sup>55</sup> to conjecture that brane formation could account for the observed air showers above the GZK cutoff<sup>103;104</sup>. Their analysis was refined by Anchordoqui et al. in Ref.<sup>56</sup> who found that cross sections of order  $\sim 100$  mb are obtained only for  $n = 1$  or  $2$ , small compactification radii, and small  $M_{\text{pl}}$ , a region of the moduli space which is excluded by experimental constraints (see Sect. 2.4). Therefore, it seems unlikely that brane formation by cosmogenic neutrinos in flat compactification models may resolve the GZK paradox. On the contrary, scenarios with warped dimensions still allow for an explanation of super-GZK events.

The current non-observation of p-brane events puts stringent limits on the fundamental scale  $M_{\text{pl}}$ . Neutrino cross sections (36) of order of a mb may enhance deep quasi-horizontal shower rates. The number of deep showers per unit time is<sup>56</sup>

$$N = \int dE N_A \frac{d}{dE} \sum_{ij} \sigma_{\text{br}}(E) A(E); \quad (91)$$

where  $N_A$  is Avogadro's number,  $d = dE$  is the neutrino flux,  $A(E)$  is the acceptance for quasi-horizontal showers in  $\text{cm}^3$  water equivalent steradians. Anchordoqui et al. have computed the event rate (91) for the AGASA experiment<sup>107</sup> and compared the result to actual data. In 1710 days of data taking, AGASA found a single deep horizontal event with an expected background of 1.72<sup>127</sup>, leading to a 95% c.l. limit of 3.5 events for brane creation. This result sets bounds both on the fundamental scale and on the size of small extra dimensions. For a number of large extra dimensions  $n \leq 4$  absence of deep quasi-horizontal showers sets the most stringent bounds on the fundamental scale  $M_{\text{pl}}$ . For  $(n; m) = (6; 5)$  and  $(n; m) = (7; 5)$  the lower bound on  $M_{\text{pl}}$  ranges from  $\sim 2 - 3$  TeV ( $L_{\text{pl}} = 2$ ) to  $\sim 0.7$  TeV ( $L_{\text{pl}} = 10L_{\text{p}}$ ). Non-observation of brane cascades at the Auger observatory<sup>108</sup> will set even more stringent bounds on  $M_{\text{pl}}$ .

Finally, Sigl<sup>128</sup> has recently given constraints on the moduli space of BH and p-brane cross sections using UHECR and neutrino data. Since brane cross sections grow slower than  $s$  (see Eq. (71)) the moduli space is not strongly constrained at energies above the TeV scale.

## 7. TeV Branes and Cosmology

In the standard cosmological scenario<sup>129</sup> and in the new brane-world cosmological models<sup>130</sup>, the temperature of the early universe is expected to have exceeded TeV values. Therefore, creation of p-branes could have been a common event in the early universe. At temperatures above the fundamental scale we expect a plasma of branes with mass  $M_{\text{p}}$  in thermal equilibrium with the primordial bath. At temperatures of order of TeV, branes decouple from the thermal plasma. If the branes are long-lived or stable, p-brane relics would appear to an observer today like heavy (supersymmetric?) particles with mass  $M_{\text{p}} \sim \text{TeV}$  and cross sections  $\sigma_{\text{br}} < \text{pb}$ , thus providing a candidate for dark matter. The presence of a gas of

branes could also solve the initial singularity and horizon problems of the standard cosmological model without relying on an inflationary phase<sup>131,132</sup>.

## 8. Conclusion and Outlook

In TeV gravity theories, processes at energies  $> \text{TeV}$  may experimentally test quantum gravitational effects. Particle collisions with CM energy larger than  $M_{\text{pl}}$  and sufficiently small impact parameter generate NPGOs: BHs, string balls and branes. Formation and subsequent decay of super-Planckian NPGO should be detectable in future particle and UHECR experiments. In cosmology, primordial creation of BHs and branes could have played an important role in the dynamics of the very early universe. Brane relics could be the dark matter which is observed today.

BH formation in LED models has attracted a lot of attention in the scientific community. The investigation of brane production is just at the beginning. Up to now, studies on brane production have focused essentially on the computation of cross sections. Brane cross sections are comparable or dominant to BH cross sections in spacetimes with at asymptotic compactifications, fat branes, and ST models. BH factories are also brane factories. On the other hand, the non-observation of BH and brane events with current UHECR detectors sets lower bounds on the fundamental scale and on the structure and size of compactified dimensions.<sup>v</sup> Eventually, either BH and brane creation will be discovered in particle collider and UHECR experiments or the fundamental scale  $M_{\text{pl}}$  will be pushed so high to make low-scale gravity models worthless.

The investigation of the theoretical and phenomenological properties of brane formation is presently limited by the ignorance of QG and the physics of gravitational collapse. Poor understanding of brane formation and decay and lack of an accurate computation of brane cross sections (both from theoretical and numerical points of view) are amongst the unsolved theoretical issues. The future studies on phenomenological implications of brane production should focus on experimental signatures in particle collider and UHECR experiments. In particular, a thorough investigation of the experimental differences between BH and brane production at particle colliders (see Sect. 3.2) is still missing. The study of cosmological and astrophysical implications of p-brane production (early universe physics, high-energy cosmic rays) is also of primary importance. BH and brane formation could play a fundamental role in all physical processes with energy above the TeV scale.

## Acknowledgements

I am very grateful to E.-J. Ahn, B. Hamers and A. O. Linto and for interesting discussions and fruitful comments, and to I. Antoniadis, U. d'Alesio, G. Dvali, J. Feng,

<sup>v</sup>Unlike BHs, p-branes which do not possess an event horizon, such as (44), do not cloak hard processes. Different hard super-Planckian processes lead to different experimental signatures which depend on the physics of the collision and on the structure of the extra dimensions.

S. Giddings, C. Giunti, H. Goldberg, R. Gregory, A. Hanany, G. Karatheodoris, S. Ponzul, J. Polchinski, Y. Uehara, A. Vilenkin and B. Zwiebach for useful comments and correspondence. This work is supported in part by funds provided by the U.S. Department of Energy under cooperative research agreement DE-FC02-94ER40818. I thank the Department of Astronomy and Astrophysics of the University of Chicago for kind hospitality.

## Appendix

We summarize other definitions of the fundamental scale that have been used in the literature.

### Giudice-Rattazzi-Wells (GRW) Notations

The observed Planck mass  $M_{Pl}$  is defined as in Eq. (2). The fundamental Planck mass is  $M_D = [\beta = (2)^n]^{-\frac{1}{n+2}} M_?$ . For a  $n$ -dimensional symmetric toroidal compactification with radii  $R$  the fundamental Planck scale is  $M_D = (8 G_4 R^n)^{-\frac{1}{n+2}}$ , where  $L = 2R$  is the length of the extra dimensions. The  $D$ -dimensional Newton constant  $G_D$  is defined as  $G_D = (2)^n = (8 M_D^{2+n})$ . GRW notations are used in Refs. <sup>13;43;54;73;74</sup>.

### Cullen-Prelstein (CP) Notations

The  $D$ -dimensional Newton's constant  $G_D$  is defined as in Eq. (7). The fundamental Planck mass  $M_D$  is defined as  $M_D = [(2)^D = 4 = (4 G_D)]^{\frac{1}{D-4}}$ . For symmetric toroidal compactifications with radii  $R$   $M_D = (4 G_4 R^n)^{-\frac{1}{n+2}} = [4 = (2)^n]^{-\frac{1}{n+2}} M_?$ . CP notations are used in Ref. <sup>27;69;72;83;84;85;86</sup>.

### Han-Lykken-Zhang (HLZ) Notations

The relation between the observed Planck mass and the fundamental scale  $M_s$  is  $M_{Pl}^2 = \frac{1}{V_n} M_s^{n+2}$ , where  $V_n = 2^{n-2} = (n=2)$  is the volume of the unit sphere in  $n-1$  dimensions. For a symmetric toroidal compactification the previous relation simplifies to  $M_{Pl}^2 = \frac{1}{R^n} M_s^{n+2}$ . The relation between  $M_s$  and  $M_?$  is  $M_s = [V_n = (2)^n]^{-\frac{1}{n+2}} M_?$ . HLZ notations are used in Refs. <sup>15;79;81</sup>.

### EOT-WASH Group Collaboration Notations

In Refs. <sup>57;58</sup> the fundamental Planck mass  $M_?$  is defined by the relation

$$R^? = \frac{1}{M_?} \frac{M_{Pl}}{M_?}^{2=n}; \quad (1)$$

where  $R^?$  is the radius of the symmetric compactification. For a toroidal compactification, setting  $R^? = L = (2)$ , we find the following relations:

$$M_? = (2)^{\frac{n}{n+2}} M_? = (8)^{\frac{1}{n+2}} M_D; \quad (2)$$

## References

1. N. Arkani-Hamed, S. Dimopoulos and G. R. Dimand, Phys. Lett. B 429, 263 (1998) [arXiv:hep-ph/9803315].
2. N. Arkani-Hamed, S. Dimopoulos and G. R. Dimand, Phys. Rev. D 59, 086004 (1999) [arXiv:hep-ph/9807344].
3. I. Antoniadis, N. Arkani-Hamed, S. Dimopoulos and G. R. Dimand, Phys. Lett. B 436, 257 (1998) [arXiv:hep-ph/9804398].
4. I. Antoniadis, Phys. Lett. B 246, 377 (1990).
5. V. A. Rubakov and M. E. Shaposhnikov, Phys. Lett. B 125, 136 (1983).
6. J. Polchinski, String Theory, Vol. I and II (Cambridge Univ. Press, Cambridge, 1998).
7. P. Horava and E. Witten, Nucl. Phys. B 475, 94 (1996) [arXiv:hep-th/9603142].
8. P. Horava and E. Witten, Nucl. Phys. B 460, 506 (1996) [arXiv:hep-th/9510209].
9. I. Antoniadis, S. Dimopoulos and A. Giveon, JHEP 0105, 055 (2001) [arXiv:hep-th/0103033].
10. K. Benakli and Y. Oz, Phys. Lett. B 472, 83 (2000) [arXiv:hep-th/9910090].
11. G. Shi and S. H. Tye, Phys. Rev. D 58, 106007 (1998) [arXiv:hep-th/9805157].
12. K. R. Dienes, E. Dudas and T. Gherghetta, Phys. Lett. B 436, 55 (1998) [arXiv:hep-ph/9803466].
13. G. F. Giudice, R. Rattazzi and J. D. Wells, Nucl. Phys. B 544, 3 (1999) [arXiv:hep-ph/9811291].
14. E. A. Mirabelli, M. Perelstein and M. E. Peskin, Phys. Rev. Lett. 82, 2236 (1999) [arXiv:hep-ph/9811337].
15. T. Han, J. D. Lykken and R. J. Zhang, Phys. Rev. D 59, 105006 (1999) [arXiv:hep-ph/9811350].
16. J. L. Hewett, Phys. Rev. Lett. 82, 4765 (1999) [arXiv:hep-ph/9811356].
17. P. C. Argyres, S. Dimopoulos and J. March-Russell, Phys. Lett. B 441, 96 (1998) [arXiv:hep-th/9808138].
18. N. Kaloper and A. D. Linde, Phys. Rev. D 59, 101303 (1999) [arXiv:hep-th/9811141].
19. L. Randall and R. Sundrum, Phys. Rev. Lett. 83, 3370 (1999) [arXiv:hep-ph/9905221].
20. L. Randall and R. Sundrum, Phys. Rev. Lett. 83, 4690 (1999) [arXiv:hep-th/9906064].
21. G. 't Hooft, Phys. Lett. B 198, 61 (1987).
22. D. Amati, M. Ciafaloni and G. Veneziano, Phys. Lett. B 197, 81 (1987).
23. D. Amati, M. Ciafaloni and G. Veneziano, Int. J. Mod. Phys. A 3, 1615 (1988).
24. H. Verlinde and E. Verlinde, Nucl. Phys. B 371, 246 (1992) [arXiv:hep-th/9110017].
25. T. Banks and W. Fischler, arXiv:hep-th/9906038.
26. S. W. Hawking, Commun. Math. Phys. 43, 199 (1975).
27. S. B. Giddings and S. Thomas, Phys. Rev. D 65, 056010 (2002) [arXiv:hep-ph/0106219].
28. S. Dimopoulos and G. Landsberg, Phys. Rev. Lett. 87, 161602 (2001) [arXiv:hep-ph/0106295].
29. K. Cheung, Phys. Rev. Lett. 88, 221602 (2002) [arXiv:hep-ph/0110163].
30. Y. Uehara, arXiv:hep-ph/0205068.
31. Y. Uehara, arXiv:hep-ph/0205199.
32. L. Anchordoqui and H. Goldberg, arXiv:hep-ph/0209337.
33. <http://lhc-new-homepage.web.cern.ch/lhc-new-homepage/>
34. <http://www.slhc.org/>
35. M. Nagano and A. A. Watson, Rev. Mod. Phys. 72, 689 (2000).
36. J. L. Feng and A. D. Shapere, Phys. Rev. Lett. 88, 021303 (2002) [arXiv:hep-ph/0109106].
37. D. Kazanas and A. Nicolaidis, arXiv:hep-ph/0109247.

38. L. Anchordoqui and H. Goldberg, Phys. Rev. D 65, 047502 (2002) [arXiv:hep-ph/0109242].
39. Y. Uehara, Prog. Theor. Phys. 107, 621 (2002) [arXiv:hep-ph/0110382].
40. M. Kowalski, A. Ringwald and H. Tu, Phys. Lett. B 529, 1 (2002) [arXiv:hep-ph/0201139].
41. J. Alvarez-Muniz, J. L. Feng, F. Halzen, T. Han and D. Hooper, Phys. Rev. D 65, 124015 (2002) [arXiv:hep-ph/0202081].
42. A. Ringwald and H. Tu, Phys. Lett. B 525, 135 (2002) [arXiv:hep-ph/0111042].
43. L. A. Anchordoqui, J. L. Feng, H. Goldberg and A. D. Shapere, Phys. Rev. D 65, 124027 (2002) [arXiv:hep-ph/0112247].
44. L. A. Anchordoqui, H. Goldberg and A. D. Shapere, Phys. Rev. D 66, 024033 (2002) [arXiv:hep-ph/0204228].
45. L. Anchordoqui, T. Paul, S. Reucroft and J. Swain, arXiv:hep-ph/0206072.
46. G. Sigl, arXiv:astro-ph/0210049.
47. R. Gregory, Nucl. Phys. B 467, 159 (1996) [arXiv:hep-th/9510202].
48. M. Cavaglia, Phys. Lett. B 413, 287 (1997) [arXiv:hep-th/9709055].
49. M. J. Du and J. X. Lu, Nucl. Phys. B 416, 301 (1994) [arXiv:hep-th/9306052].
50. M. J. Du, H. Lu and C. N. Pope, Phys. Lett. B 382, 73 (1996) [arXiv:hep-th/9604052].
51. K. S. Stelle, arXiv:hep-th/9701088.
52. E. J. Ahn, M. Cavaglia and A. V. Olinto, arXiv:hep-th/0201042.
53. E. J. Ahn and M. Cavaglia, arXiv:hep-ph/0205168.
54. K. Cheung, Phys. Rev. D 66, 036007 (2002) [arXiv:hep-ph/0205033].
55. P. Jain, S. Kar, S. Panda and J. P. Ralston, arXiv:hep-ph/0201232.
56. L. A. Anchordoqui, J. L. Feng and H. Goldberg, Phys. Lett. B 535, 302 (2002) [arXiv:hep-ph/0202124].
57. C. D. Hoyle, U. Schmidt, B. R. Heckel, E. G. Adelberger, J. H. Gundlach, D. J. Kapner and H. E. Swanson, Phys. Rev. Lett. 86, 1418 (2001) [arXiv:hep-ph/0011014].
58. E. G. Adelberger [EOT-WASH Group Collaboration], arXiv:hep-ex/0202008.
59. I. Antoniadis and B. P. Ioline, arXiv:hep-ph/9906480.
60. I. Antoniadis and B. P. Ioline, Nucl. Phys. B 550, 41 (1999) [arXiv:hep-th/9902055].
61. J. D. Lykken, Phys. Rev. D 54, 3693 (1996) [arXiv:hep-th/9603133].
62. I. Antoniadis, arXiv:hep-th/0102202.
63. S. Forste, Fortsch. Phys. 50, 221 (2002) [arXiv:hep-th/0110055].
64. H. Verlinde, Nucl. Phys. B 580, 264 (2000) [arXiv:hep-th/9906182].
65. S. B. Giddings, S. Kachru and J. Polchinski, arXiv:hep-th/0105097.
66. J. Lykken and S. Nandi, Phys. Lett. B 485, 224 (2000) [arXiv:hep-ph/9908505].
67. N. Arkani-Hamed and M. Schmaltz, Phys. Rev. D 61, 033005 (2000) [arXiv:hep-ph/9903417].
68. T. Appelquist, H. C. Cheng and B. A. Dobrescu, Phys. Rev. D 64, 035002 (2001) [arXiv:hep-ph/0012100].
69. M. E. Peskin, arXiv:hep-ph/0002041.
70. Y. Uehara, arXiv:hep-ph/0203244.
71. K. M. Cheung, arXiv:hep-ph/0003306.
72. S. Cullen, M. Peralstein and M. E. Peskin, Phys. Rev. D 62, 055012 (2000) [arXiv:hep-ph/0001166].
73. M. Acciarri et al. [L3 Collaboration], Phys. Lett. B 470, 268 (1999) [arXiv:hep-ex/9910009].
74. M. Acciarri et al. [L3 Collaboration], Phys. Lett. B 464, 135 (1999) [arXiv:hep-ex/9909019].

75. R. Barate et al. [ALEPH Collaboration], Phys. Lett. B 429, 201 (1998).
76. P. Abreu et al. [DELPHI Collaboration], Phys. Lett. B 485, 45 (2000) [arXiv:hep-ex/0103025].
77. G. Abbiendi et al. [OPAL Collaboration], Eur. Phys. J. C 13, 553 (2000) [arXiv:hep-ex/9908008].
78. C. Adlb et al. [H1 Collaboration], Phys. Lett. B 479, 358 (2000) [arXiv:hep-ex/0003002].
79. B. Abbott et al. [D0 Collaboration], Phys. Rev. Lett. 86, 1156 (2001) [arXiv:hep-ex/0008065].
80. S. Cullen and M. Perelstein, Phys. Rev. Lett. 83, 268 (1999) [arXiv:hep-ph/9903422].
81. V. D. Barger, T. Han, C. Kao and R. J. Zhang, Phys. Lett. B 461, 34 (1999) [arXiv:hep-ph/9905474].
82. C. Hanhart, J. A. Pons, D. R. Phillips and S. Reddy, Phys. Lett. B 509, 1 (2001) [arXiv:astro-ph/0102063].
83. S. Hannestad and G. Raelt, Phys. Rev. Lett. 87, 051301 (2001) [arXiv:hep-ph/0103201].
84. S. Hannestad and G. G. Raelt, Phys. Rev. Lett. 88, 071301 (2002) [arXiv:hep-ph/0110067].
85. M. Fairbairn, Phys. Lett. B 508, 335 (2001) [arXiv:hep-ph/0101131].
86. L. J. Hall and D. R. Smith, Phys. Rev. D 60, 085008 (1999) [arXiv:hep-ph/9904267].
87. S. Dimopoulos and R. Emparan, Phys. Lett. B 526, 393 (2002) [arXiv:hep-ph/0108060].
88. P. D. D'Eath and P. N. Payne, Phys. Rev. D 46, 658 (1992).
89. P. D. D'Eath and P. N. Payne, Phys. Rev. D 46, 675 (1992).
90. P. D. D'Eath and P. N. Payne, Phys. Rev. D 46, 694 (1992).
91. E. Kohlhprath and G. Veneziano, JHEP 0206, 057 (2002) [arXiv:gr-qc/0203093].
92. S. C. Park and H. S. Song, arXiv:hep-ph/0111069.
93. S. N. Solodukhin, Phys. Lett. B 533, 153 (2002) [arXiv:hep-ph/0201248].
94. M. B. Voloshin, Phys. Lett. B 518, 137 (2001) [arXiv:hep-ph/0107119].
95. M. B. Voloshin, Phys. Lett. B 524, 376 (2002) [arXiv:hep-ph/0111099].
96. <http://www.pam.su.edu/hep/cteq/cteq6/>
97. R. Casadio and B. Hamers, arXiv:hep-th/0110255.
98. R. Emparan, G. T. Horowitz and R. C. Myers, Phys. Rev. Lett. 85, 499 (2000) [arXiv:hep-th/0003118].
99. T. Han, G. D. Kribs and B. McElrath, arXiv:hep-ph/0207003.
100. T. G. Rizzo, in Proc. of the APS/DPF/DPB Summer Study on the Future of Particle Physics (Snowmass 2001) ed. R. Davidson and C. Quigg, arXiv:hep-ph/0111230.
101. T. G. Rizzo, JHEP 0202, 011 (2002) [arXiv:hep-ph/0201228].
102. R. Engel, D. Seckel and T. Stanev, Phys. Rev. D 64, 093010 (2001) [arXiv:astro-ph/0101216].
103. K. G. Reisen, Phys. Rev. Lett. 16, 748 (1966).
104. G. T. Zatsarin and V. A. Kuzmin, JETP Lett. 4, 78 (1966) [Pisma Zh. Eksp. Teor. Fiz. 4, 114 (1966)].
105. M. Bleicher, S. Hofmann, S. Hossenfelder and H. Stoecker, arXiv:hep-ph/0112186.
106. S. Hofmann, M. Bleicher, L. Gerland, S. Hossenfelder, K. Paech and H. Stoecker, J. Phys. G 28, 1657 (2002).
107. <http://www.akeno.icrr.u-tokyo.ac.jp/AGASA/>
108. <http://www.auger.org/>
109. M. Cavaglia, B. Hamers and G. Karatheodoris, unpublished.
110. See, e.g., C. Misner, K. S. Thorne and J. A. Wheeler, Gravitation (W. H. Freeman,

New York,1973)

111. J. X. Lu, Phys. Lett. B 313, 29 (1993) [arXiv:hep-th/9304159].
112. K. Cheung and C. H. Chou, Phys. Rev. D 66, 036008 (2002) [arXiv:hep-ph/0205284].
113. K. S. Stelle, Given at APCTP Winter School on Dualities of Gauge and String Theories, Seoul and Sokcho, Korea, 17-28 Feb 1997.
114. A. Sen, Int. J. Mod. Phys. A 14, 4061 (1999) [arXiv:hep-th/9902105].
115. A. Sen, arXiv:hep-th/9904207.
116. A. Sen, JHEP 9912, 027 (1999) [arXiv:hep-th/9911116].
117. S. Moriyama and S. Nakamura, Phys. Lett. B 506, 161 (2001) [arXiv:hep-th/0011002].
118. L. Rastelli, A. Sen and B. Zwiebach, Adv. Theor. Math. Phys. 5, 353 (2002) [arXiv:hep-th/0012251].
119. T. Lee, Phys. Lett. B 520, 385 (2001) [arXiv:hep-th/0105264].
120. T. Lee, Phys. Rev. D 64, 106004 (2001) [arXiv:hep-th/0105115].
121. D. M. Eardley, G. T. Horowitz, D. A. Kastor and J. Traschen, Phys. Rev. Lett. 75, 3390 (1995) [arXiv:gr-qc/9506041].
122. S. W. Hawking and S. F. Ross, Phys. Rev. Lett. 75, 3382 (1995) [arXiv:gr-qc/9506020].
123. R. Gregory and M. Hindmarsh, Phys. Rev. D 52, 5598 (1995) [arXiv:gr-qc/9506054].
124. H. Iguchi and T. Harada, Class. Quant. Grav. 18, 3681 (2001) [arXiv:gr-qc/0107099].
125. M. Cavaglia, G. Karatheodoris and B. Harris, in preparation.
126. A. Chamblin, S. W. Hawking and H. S. Reall, Phys. Rev. D 61, 065007 (2000) [arXiv:hep-th/9909205].
127. S. Yoshida et al. [AGASA Collaboration], in Proc. 27th International Cosmic Ray Conference, Hamburg, Germany, 2001, Vol. 3, p. 1142.
128. G. Sigl, arXiv:hep-ph/0207254.
129. See, e.g., E. W. Kolb and M. S. Turner, The Early Universe (Perseus Publishing, Cambridge MA, 1994)
130. J. Khoury, B. A. Ovrut, P. J. Steinhardt and N. Turok, Phys. Rev. D 64, 123522 (2001).
131. S. Alexander, R. H. Brandenberger and D. Easson, Phys. Rev. D 62, 103509 (2000).
132. R. Brandenberger, D. A. Easson and D. Kinberly, Nucl. Phys. B 623, 421 (2002).